Simulation of Enviro-mechanical Durability for Life Prediction of E-Glass/Vinyl Ester Composites using a Bridge Service Environment

By

David Alan Jungkuist

Thesis submitted to the Faculty of the
Virginia Polytechnic Institute and State University
In partial fulfillment of the requirements for the degree of

Master of Science
in
Engineering Mechanics

John J. Lesko, Chair
Scott Case
David Dillard

December 12, 2000

Blacksburg, Virginia Tech

Keywords: Glass Composites, Fatigue, Environmental Durability, Life Prediction, and Moisture Diffusion

Simulation of Environ-mechanical Durability for Life Prediction on E-Glass/Vinyl Ester Composites using a Bridge Service Environment

David Alan Jungkuist

John J. Lesko, Chair

Engineering Science & Mechanics

(ABSTRACT)

In order for composites to become an accepted material for infrastructure application, life prediction and durability must be understood. The majority of studies have examined the strength and fatigue response of composites under hot and/or moist conditions. Various researchers have also studied life prediction methods for composite materials under fatigue, primarily for high performance applications. Little work has been done to study durability under combined service conditions for composites used in civil infrastructure applications.

This thesis focuses on the development of a life prediction model for use with fiber reinforced polymer composites in bridge service environments. The Tom's Creek Bridge of Blacksburg, VA is used as a guiding case study. First, the tensile properties of the composite were studied as a function of temperature and moisture. Damage accumulation was studied as a function of cyclic loading and temperature cycles. The enviro-mechanical conditions, including moisture, temperature and fatigue loading, were then used in a computer simulation to predict the life of a vinyl ester/glass composite under an approximate bridge service environment.

Finally, a laboratory simulation was conducted that approximates the temperature and humidity that is seen at the Tom's Creek Bridge, but in an accelerated time frame. A multi-stress fatigue pattern, mimicking cars and trucks passing over the bridge, was used. One year of conditions was accelerated to approximately six hours and thirty-three minutes using a servo-hydraulic test frame and environmental chamber.

The final results showed that life prediction methodology conservatively predicted the lifetime of a vinyl ester/glass composite under the enviro-mechanical conditions. The damage of the composite was predominately driven by cyclic loading. The environmental conditions of moisture and temperature had only a small affect on the lifetime of the composite. This lack of environmental sensitivity is largely due to the durability of the resin system.

DEDICATION

"A teacher came to class with an empty glass mason jar and began filling it with large rocks. When the rocks reached the top of the jar he asked the class if the jar was full. A student answered yes. The teacher then added gravel to the jar and asked the same question, "Is the jar full?" Another student, wising up to the situation said, "No." Smiling from the correct answer, the teacher added sand to the jar, and upon finishing asked the question, "Is this jar now full?" The class responded with another no. The teacher then brought out a pitcher of water and filled the jar. He then asked if the jar was full. Not knowing what else could be placed in the jar, the class could only answer with silence. The teacher interrupted the silence by saying that the jar was indeed full. Then the teacher asked his class what the moral of the demonstration was. An eager student quickly responded that the demonstration shows that you can always find more room for responsibilities. Shaking his head no, the teacher explained that in life you have many different size responsibilities and that you must first put in the big rocks, or they will never fit in the jar."

This work is dedicated to the *big rocks* of my life. Thanks to my wife, Robbie, son Dominic, my parents, Larry and Teri, my brothers, Steve and John, and my family-in-law, John, Dianne and Jason Laurence. Your love and patience has been the key to my academic success.

ACKNOWLEDGMENTS

I wish to acknowledge the following individuals whose support and contributions led to the success of this work.

The Committee

- **Dr. John "Jack" Lesko** – thank you for your immense contributions to both my academic and research success. Not only have you served as my advisor, but a role model and friend as well.
- **Dr. Scott Case –** thank you for your tremendous assistance in getting my computer simulation off of the ground. I appreciate your willingness to help. I hope that you continue to find your joys in life, and never lose that outside jumper.
- **Dr. David Dillard –** thank you for bringing me to Virginia Tech as a part of the Summer Undergraduate Research Program. The people and this area have made a dramatic impact on my life that I will always remember and hold.

The Materials Response Group

- **Steve Phifer** – thank you for all of your help. My thesis title should have you as a second author. I also appreciate your willingness to lend an ear. Your advice has turned frustrating days into sunshine. And lastly, thank you for the baby crib and stroller in support of my new family addition.
- **Dr. Nikhil Verghese** – thank you for your friendship and inspiration. I still remember the SURP days and our big volleyball win during the CASS picnic.
- **Dr**. **Byung-Kim Ahn –** thank you for all of your smiles and support as I prepared for fatherhood. I hope that you enjoy your stay in the state of Washington.

- **John Haramis –** thank you for your help with freezing and thawing… everything.
- **Tozer Bandorawalla –** thank you for all of the laughter. Your voice will ring through Patton Hall for years. I hope that our paths will cross again in the future.
- **Dr. Howard Halverson –** thank you for all of your materials testing help. I could not have broken so many things without your help.
- **Sneha Patel** – thank you for your patience and sharing of the environmental chamber. Also, thank you for letting Lester stay with us.
- **Mac McCord –** thank you for pulling me out of my various testing jams. Both the MRG and myself are forever in your debt.
- **Beverly Williams and Shelia Collins –** two of the best secretaries in the world. The MRG would never run without the guidance of you. Thank you for all of your help.
- **Michael Pastor –** Not only an engineer, but a fellow underwater hockey player. Thank you for your friendship and all of the study breaks.
- **Joe South** - Not only do you possess a great knowledge of engineering, you also possess a pretty good golf swing. Thank you for all the good times on the links.
- **David Haeberle –** thank you for your friendship. You have a wonderful personality and a contagious smile.
- **Jason Burdette** – You are one of the most focused individuals that I have ever met. I know that you will succeed in everything you set your mind too.
- **Rob Carter –** the resident grandfather of the MRG. Thank you for all of the MRG specials at "Top of the Stairs."
- **Blair Russell –** thank you for your friendship and knowledge of sushi.
- **Jolyn Senne –** the queen bee of the MRG. There are few people with the work ethic that you possess. It is an inspiration.
- **Nadia Oubechou –** thank you for your friendship. I hope that our paths cross again some day.
- **Daniel Graves –** President of the Underwater Hockey Club of Virginia Tech, fellow scientist, engineer and friend. Thank you for initiating me into the craziest sport of all. I hope to see you soon on the bottom of a pool.

Engineering Science and Mechanics Dept.

- **Pat Baker –** thank you for your patience with my organizational skills.
- **Wanda Robertson–** thank you for helping me with purchase orders. I hope that you enjoy your retirement. You will be missed.
- **Loretta Tickle –** thank you for keeping the E.S.M. department running. I always enjoyed dropping by and talking about everything from Abyssinian cats to how to be a father.
- **Bob Simonds** – thank you for your immense contributions to my experimental work. I also appreciate your willingness to lend a hand when machines went down. I would never have graduated without your help.
- **George Lough** – thank you for your help with keeping the hydraulic systems working.

Undergraduate Support

- **Amy Mell –**Thank you for your help and dedication. I would not have survived the summer of 1998 without your support.
- **Matt Gunzburger** – I appreciate your help with the NIST project, especially with the polishing of samples.
- **James Fazio –** thank you for your dedication and friendship. You are one of the hardest workers that I have ever seen. I look forward to seeing how you continue this study.

TABLE OF CONTENTS

LIST OF FIGURES

LIST OF TABLES

Chapter 1. Introduction and Objectives

1.1. Introduction

Polymer matrix composite (PMC) materials came about due to the need for high strength to weight materials. Thirty years ago, this need for high strength to weight materials was in the aerospace industry, where every ounce saved improves performance. Thus, the aerospace industry spent time and money creating high performance composite materials. With the success in aerospace, composite technology began to be a viable material solution in other applications, such as cars, marine, sports and recreation, and infrastructure. Unlike the aerospace industry, cost played an important role.

The evolution of composites in infrastructure is the result of national concerns with regard to the numbers of deteriorating bridges in the United States. In infrastructure, strength to weight is not necessarily seen as a critical design parameter. This is easily observed since current steel and concrete structures are quite heavy. Instead, polymer composites offer increased corrosion resistance. Their lighter weight structures help by reducing dead load, and decreasing installation time.

The total number of bridges in the U.S. is reported to be between 540,000 and 600,000. Approximately 5-10% of these bridges are considered to be in a state of advanced decay with immediate need for repair [1]. One source indicates that as many as 200,000 are either “structurally deficient” or “functionally obsolete [2].” The cost per year to rehabilitate these bridges is enormous, estimated at around $80 billion [3]. According to a report by the Great Lakes Composites Consortium (GLCC), the Basic Industrial Research Laboratory (BIRL), Northwestern University, and the University of Kentucky, a typical bridge lifespan is estimated at 70 years [4]. Also detailed in the report is that the average bridge requires rehabilitation at mid-life due to deterioration with most of the damage caused by corrosion of the bridge deck due to deicing salts. The majority of the bridges in the U.S. were built after 1945 and it is estimated that 40% will need to be replaced within 10 years [5]. With this growing need for bridge repair,

rehabilitation, and replacement, new materials such as composites are being looked at to possibly decrease costs, improve durability, and lengthen lifetimes.

Polymeric composites offer many advantages over their concrete and metal counterparts including corrosion resistance, and higher strength to weight ratio. A lighter structure, a feature offered by composites, offers many advantages. The dead load of the structure is significantly reduced, allowing for larger factors of safety. Lighter materials allow for quicker installation. These structures can be produced before installation. While it can take up to a month for a concrete bridge to cure, a composite bridge can be in service almost immediately.

Unfortunately, a major disadvantage for composite materials is cost. Current cost of concrete and rebar structures is measured in the pennies per pound, 2 and 12 cents per pound for concrete and rebar respectively, while infrastructure grade composites range in the dollars per pound [5]. Examples of composites used in infrastructure include glass fiber with epoxy, polyester, or vinyl ester matrices. Although initial material costs are high, they are reduced by faster installation, rehabilitation, and maintenance. Another major drawback that composites are seeing in infrastructure applications is a lack of data supporting composite durability. Although prices of composites will decrease as technology increases, in order for composites to sell in this industry, durability studies must show the value of the increase in cost. One technology that produces relatively inexpensive composites is the pultrusion process.

Composites are under criticism in the infrastructure industry. Although they offer many advantages over steel and concrete structures, their cost is an order of magnitude higher (concrete and steel prices are measured in the pennies per pound, while composites are dollars per pound). Another criticism is durability of composite materials. Concrete and steel structures have been used for over a hundred years, and thus are well-understood materials. Infrastructure composites, on the other hand, are still in their infancy.

As technology develops, the cost of composites will decrease. Currently, many researchers are studying the durability and life prediction of composite materials under various environmental conditions. The challenge will be the acceptance of these materials as a viable alternative to past technology.

1.2. Durability and Life Prediction of Composites: Motivation

One of the major obstacles that composites are facing in infrastructure applications is the issue of durability and life prediction. Different sources indicate that a composite bridge must guarantee 50-100 years of service life before installation is accepted [5]. This is a longer expected service life than that used in the aerospace industry. At this time, the infrastructure industry has focused predominantly on lower-cost glass reinforcement rather than the carbon fiber reinforcement used in aerospace applications. As a result, experience gained from the past may serve as a guideline. Thus, new studies and data pertaining to infrastructure applications are in great demand.

Environmental durability is of great concern for composite materials used in infrastructure. Bridges will not only be subjected to variable loading from cars and trucks, but must withstand high and low temperatures, moisture, salt water, and ultraviolet radiation. In recent years, many researchers have been analyzing the different aspects that fall under the category of environmental durability. Springer et al. have studied the effect of temperature and moisture on composite materials [6-15]. As shown by the number of references given here, Springer and his colleagues have looked at the environmental durability from a variety of angles. For a large part, these studies have looked at environmental durability under accelerated conditions by elevating temperature under humid environments or water bath ageing. This trend in studying environmental durability under hot and moist conditions is continued by other researchers. Singhal and Chamis analyzed long term environmental durability under hot and humid service conditions by including creep studies [16]. Accelerated environmental testing has been studied by Ciriscioli et al. in which rapid moisture absorption methods are shown [17]. Sridharan completed his doctorate degree with a study on environmental durability of pultruded E-Glass/vinyl ester composites under hot-moist conditions [18]. Chateauminois et al. analyzed the fatigue response of glass/epoxy composites under hygrothermal ageing conditions [19]. Strength and fatigue response are also a function of temperature. Studies by Jungk et al. showed a change in both strength and slope of the

normalized S-N curve with response to change in temperature in vinyl ester/E-glass composites [20]. The results showed an 8% decrease in strength and an increase in slope from 7.5 to 12 % strength per decade of life between 0 and 65° C.

In colder temperatures, environmental durability may actually improve. The strength of a glass fiber composite increases, moisture diffusion decreases, and degradation mechanisms decrease. Thus, environmental durability issues seen in hot-moist conditions are not as prevalent. Instead, freeze thaw cycles are of greater concern for the lifetime of a composite material. Original freeze-thaw studies stemmed from concrete structures where moisture absorbed into the material, then under freezing conditions, the moisture expanded and created cracks. This has also been documented in glass reinforced polymer composites. Gomez and Castro [21] subjected both polyester and vinyl ester composites to temperature cycles (0° to 40° F) under a 2% salt-water solution. A 20% reduction in strength was seen at 300 freeze-thaw cycles. Thermal cycling between –60° and 60° C of S-2/epoxy composites was studied by Dutta [22]. Studies by Haramis [23] have shown a decrease in strength in pultruded vinyl ester/E-glass composites due to cyclic temperatures.

One can find much information on the individual mechanisms regarding environmental durability of composite materials, but few studies have looked at combined environments of load, temperature, and humidity. To date, there has not been a study to mimic service conditions of infrastructure where composite materials are being used. The goal of this thesis is to bridge these different environmental studies together by creating a life prediction model. Laboratory simulations of bridge service conditions are conducted, using conditions seen at the Tom's Creek Bridge of Blacksburg, VA as a test case.

1.3. Objectives

This thesis focuses on the development of a life prediction model for use with fiber reinforced polymer composites in bridge service environments. This will be accomplished by creating a computer simulation based on the conditions seen at the Tom's Creek Bridge of Blacksburg, VA. A laboratory simulation will also be performed to validate the findings of the computer simulation. Secondary goals include determining strength and modulus of a vinyl ester/E-glass composite as a function of moisture and temperature, and damage as a function of cyclic temperature and fatigue cycles.

Chapter 2. Literature Review

2.1. Pultruded Composites

The pultrusion process of composites is analogous to the extrusion process of thermoplastic or aluminum materials. In the pultrusion process, fibers are pulled through a system that first applies a resin then cures the resin in a heated die as shown in Figure 1. The finished product has a constant cross sectional area. Currently, unidirectional, woven, and stitched fabric fibers are available thus allowing to make cross-ply and quasi-isotropic laminates. Another variation of this technique is the continuous resin transfer molding (CRTM) process (Figure 2). Instead of using a resin bath, the resin is injected into the dry fiber. This reduces the fiber distortion caused by fiber lubricity. Also, hydraulic pressures at the die entrance squeeze excess resin from the composite. This method prevents addition of fillers, since the compressed fiber reinforcement acts as a dense filter, hindering filler penetration.

Polyester/glass composites are the most common material combination seen in pultruded composites. Glass has a much lower cost than carbon, while polyester has a low viscosity for easier penetration. Vinyl ester is the next highest volume resin seen. It has similar chemistry and processing to polyester. The increased toughness, corrosion resistance, and heat distortion properties supplement vinyl ester's higher cost and slower cure time. Epoxy resins are used the least due to their higher cost, slower cure rates, and cure shrinkage problems. Epoxies do offer the best long-term electrical and hygrothermal properties.

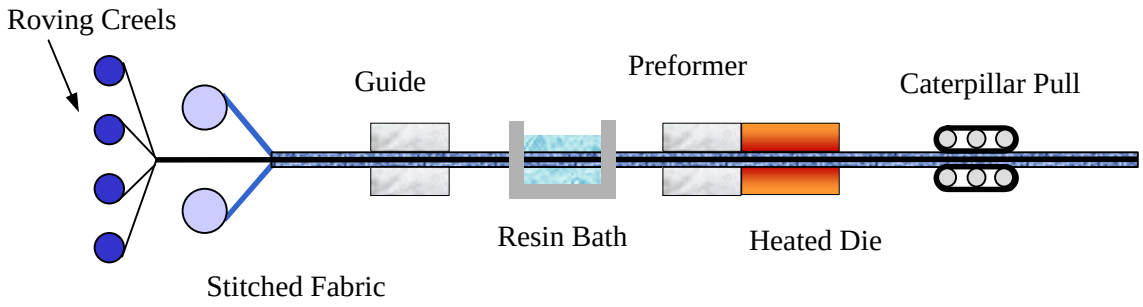

Figure 1. Resin Bath Pultrusion Process

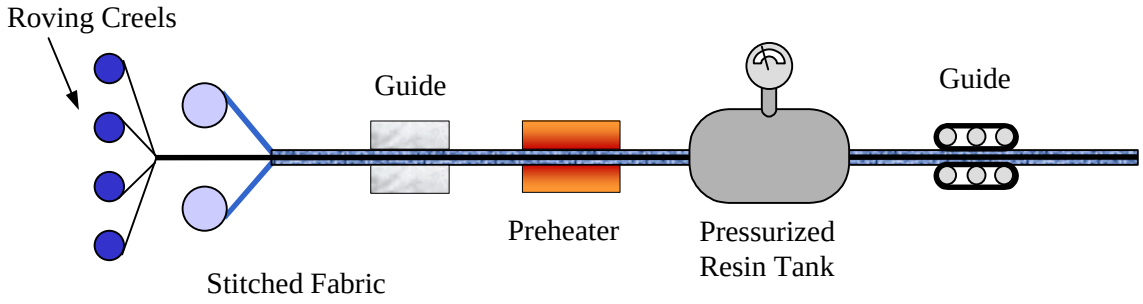

Figure 2. Continuous Resin Transfer Molding Process

The advantages of the pultrusion process include elimination of process support materials such as bagging and breather materials seen in hand lay-up operations, low materials scrap by product, and low labor costs. Since they are pulled through a die, their shape is limited to constant cross sections. These composites have found applications in the electrical equipment market, transportation industry in the form of bumpers, frames, and drive shafts as well as the construction industry in the form of gratings, guard rails, platforms and bridges.

2.2. Environmental Factors Affecting Composite Properties

The increasing use of fiber reinforced polymer composites in structural applications requires the response to environmental exposure be understood. Environmental factors analyzed in this study include temperature, freeze-thaw cycles, and moisture. These conditions were analyzed with and without the presence of fatigue load. Ultraviolet (UV) radiation, salt water, and gasoline are examples of other exposures that can degrade composite bridge properties, but will not be evaluated in this study.

2.2.1. Temperature

Materials expand or contract upon temperature change. The amount of contraction, or expansion, can be determined by multiplying the coefficient of thermal expansion (CTE), denoted by α, and the change in temperature. Composite manufacture is often completed at elevated temperatures. It is not uncommon for a composite to see a change in temperature of –150°C from processing to room temperature. Thus internal stresses are established in the material even before an external load is applied. This is commonly observed in pultruded composites in the form of matrix cracking.

Owens Corning reported that the fiber tensile strength changes as a function of temperature [27]. Figure 3 shows the tensile strength of various fibers as a function of temperature. The results show that during service conditions of a bridge, defined by the Tom's Creek Bridge as 0°-100° F in this study, there is less than a 10% change in the strength.

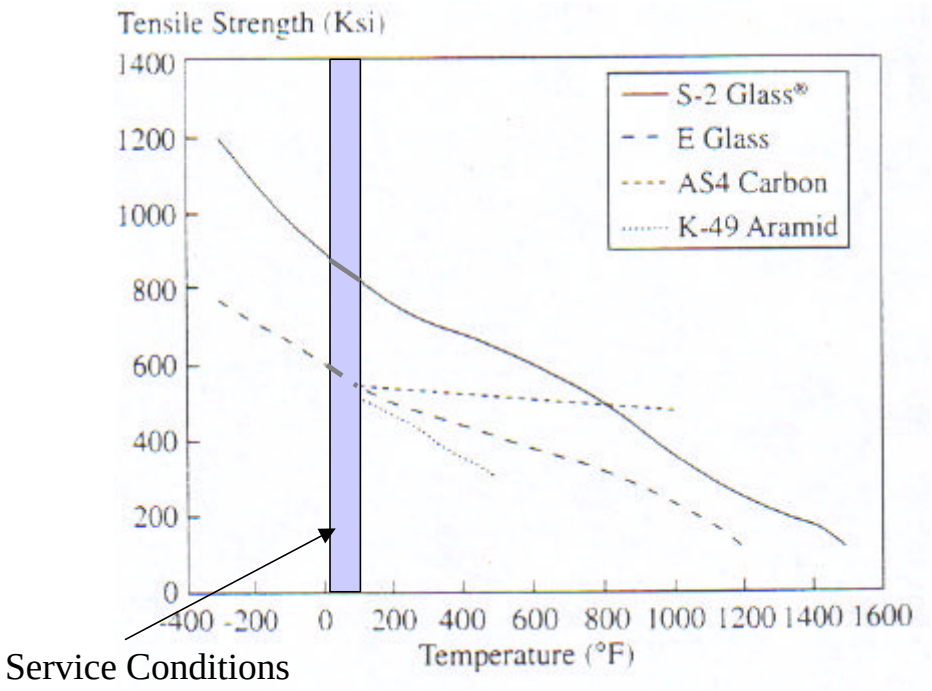

Figure 3. Tensile strength of various fibers as a function of temperature. Note that the change in strength is relatively small (less than 10% change) [27].

Phifer et al. performed quasi-static tensile tests at a range of temperatures from -55° to 90° C on a neat vinyl ester resin, vinyl ester/glass cross-ply composite and vinyl ester/glass angle-ply composite [28]. The results of these experiments can be seen in Figure 4 and Figure 5. Under reasonable terrestrial bridge service conditions, no change in strength of cross-ply vinyl ester/glass composites or neat resin was seen. Similar trends are seen in data for modulus as a function of temperature where there was no change in modulus of the cross ply and angle ply composite over bridge service conditions. There is a significant change in neat resin modulus over bridge service condition temperatures. Although this change in modulus will not greatly effect the composite modulus in the fiber direction, it will noticeably change the transverse composite ply modulus. In the case of a cross ply laminate, the transverse modulus of the 90° plies will vary due to the change in neat resin modulus. This modulus change will then redistribute the stress state of the material, including the stress on the 0° fibers.

Ply modulus can be modeled from the neat resin modulus using Halpin-Tsai micromechanics (equations 4 and 5).

$$\frac{E_2}{E_2(matrix)} = \frac{1+hzV_f}{1-hV_f} \tag{1}$$

$$h = \frac{\left(E_2(fiber)/E_2(matrix)\right)-1}{\left(E_2(fiber)/E_2(matrix)\right)+z} \tag{2}$$

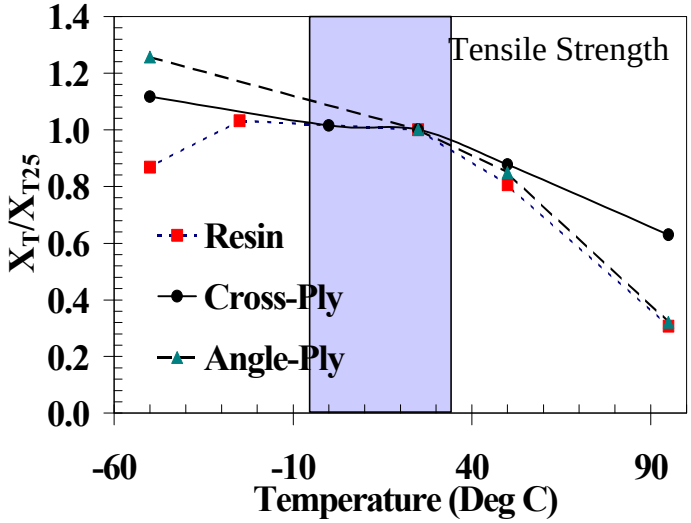

Figure 4. Normalized tensile strength as a function of temperature for the neat resin matrix, vinyl ester/glass composite cross-ply and angle-ply [28].

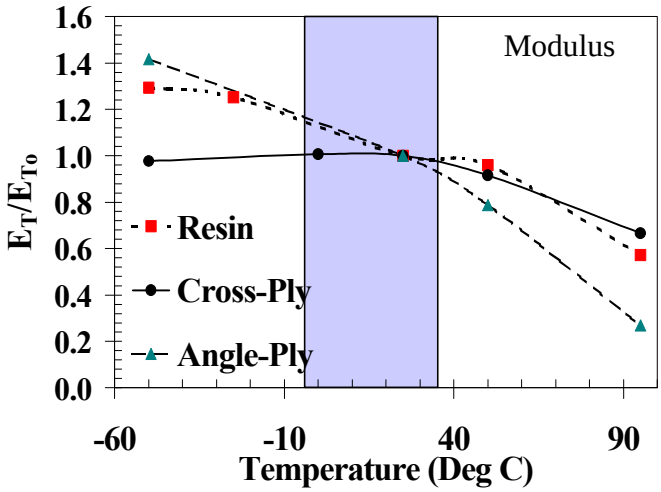

Figure 5. Normalized modulus as a function of temperature for the neat resin matrix, vinyl ester/glass composite cross-ply and angle-ply [28].

Cyclic temperature is also considered as a possible damage mechanism. Henaff-Gardin et al. compared cyclic temperature to mechanical loading and attempted to mimic the effects of cyclic loading with mechanical loading [29, 30]. This work was done with the cross-ply laminate. The effect of changing temperature can best be explained using a pictograph of Figure 6. Since thermal expansion in the transverse direction of a composite is greater than the fiber direction, an increase in temperature will create a large free expansion in the transverse direction. Due to bonding between layers, each layer will not be allowed to freely expand. The result is a biaxial load with a tensile load in the fiber direction and a compressive load in the transverse direction. During cyclic loading, these values change and the results can be similar to mechanical fatigue. X-radiographs were used to measure crack densities in the 0° and 90° plies. Crack densities were seen to reach a saturation value within ten cycles for –200 to 20°C temperatures.

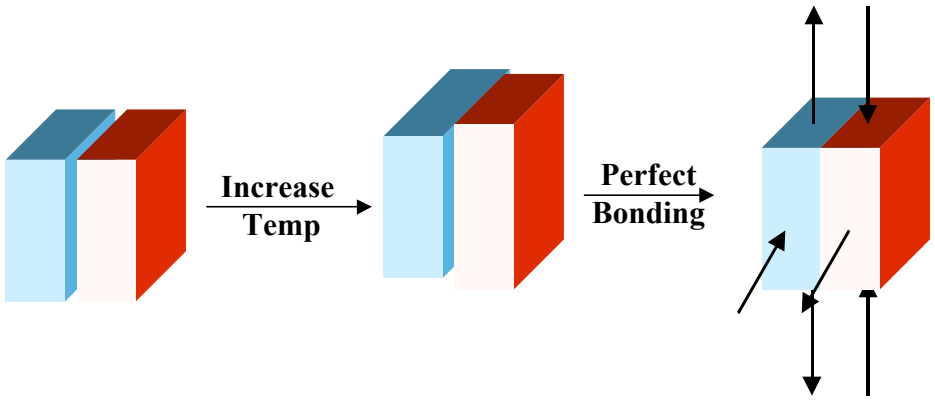

Figure 6. For a cross-ply composite, increasing temperature causes a biaxial stress state for each ply.

Thermally induced fractures have also studied by Fang, Shapery, and Weitsman [31]. Fang et al. worked with graphite epoxy cross-ply composites. Instead of cyclic temperatures, they brought the composite from cure temperatures to various temperatures (ΔT of –217 to –369 K) under rapid and slow (3 K per minute) cooling rates. The results showed that early stages of slow thermal excursions created crack patterns similar to mechanical loading effects. These crack patterns could be modeled using a 2-D micro-cracking model. Rapid cooling developed curved cracks and free-edge delaminations.

2.2.2. Freeze/Thaw Cycles

Freeze/thaw cycles are defined as cyclic temperature that crosses the freezing point of water. Literature suggests that freeze/thaw cycles can create damage in the form of matrix and/or fiber cracks [21], [23]. The idea is that moisture in the composite freezes and expands, creating cracks. Currently there is debatable evidence at whether freeze/thaw cycles are the dominant damage mechanism. Experimental results from Haramis mentions that the cyclic temperature may in fact be the dominant damage mechanism [23]. Haramis studied specimens that were loaded and unloaded as well as dry and saturated with moisture. These four different conditions were then subjected to thermal cycling between –17.8° and 30°C. The results in Figure 7 show that both dry and saturated composites showed little strength degradation from thermal cycling in the unloaded case, but relatively the same amount of degradation in the loading situation. This implies that moisture freezing, with subsequent crack formation, isn't the driving mechanism for strength reduction.

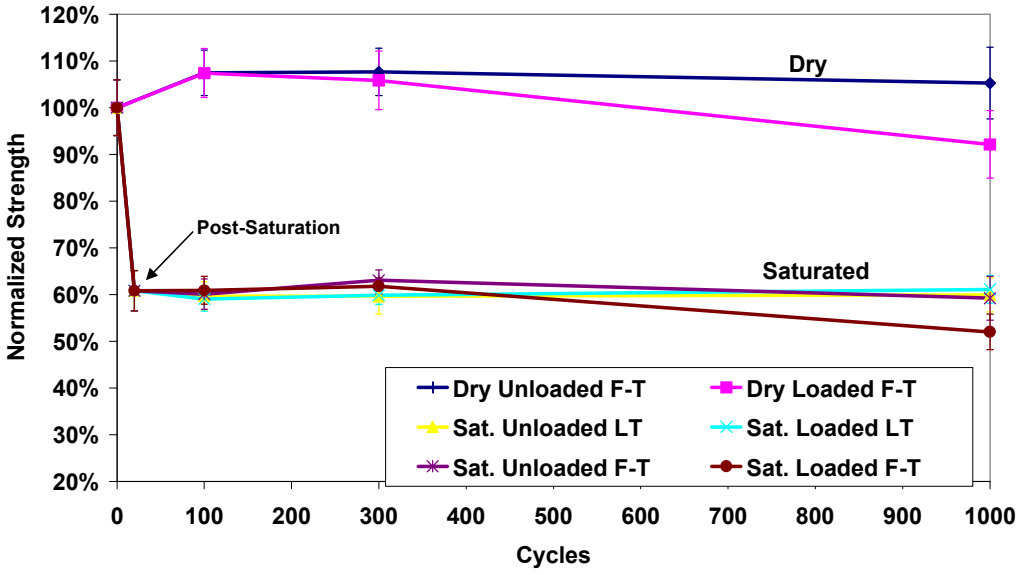

Figure 7. The effects of freeze/thaw cycles on loaded and unloaded vinyl ester/glass composite [23].

2.2.3. Moisture

There are numerous studies on the effects of moisture on composite materials. These effects can be within the matrix, on the fiber, at the fiber-matrix interface, or on the composite. Moisture can act as a plasticizer, thus reducing the matrix modulus. Literature has also shown that moisture can increase crack density, which would also have an effect on the modulus. Moisture can attack the fiber during loading causing stress-corrosion cracking. Cracks can form at the fiber-matrix interface, thus decreasing the stress transfer of the composite (Figure 8).

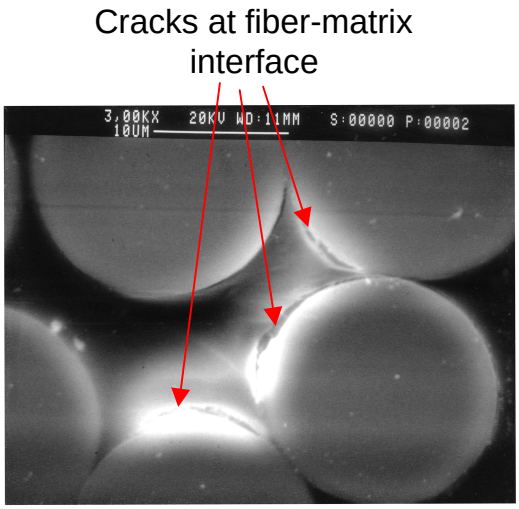

Figure 8. Cracks formed at the fiber-matrix interface from moisture.

The properties of a composite exposed to water are a function of the concentration. The concentration is dependent upon temperature, exposure time, and material properties (i.e. diffusion coefficient and activation energy). Diffusion is defined as the process by which matter is transported from one part of a system to another as a result of random molecular motion. Although diffusion is defined as random, due to net transfer of particles, motion moves from areas of high to low concentration. Fick was the first to recognize this phenomenon for net transfer of particles and quantitatively defined diffusion using Fourier's heat conduction equation.

$$\frac{\partial T}{\partial t} = a \frac{\partial^2 T}{\partial x^2} \qquad (3)$$

Where temperature (T) is a function of time (t) and distance (x) and heat conduction (α) is given as:

$$a = \frac{k}{\rho c_p} \tag{4}$$

Hence, Fick's law has a similar form to Fourier's heat conduction equation.

$$\frac{\partial c}{\partial t} = D\frac{\partial^2 c}{\partial x^2} \tag{5}$$

Where c is the concentration as a function of time (t) and x (distance through the material) and D is the diffusion constant. The diffusion constant and heat conduction are measures of the speed of moisture and temperature changes. A ratio of α over D would give a value of 10^5 to 10^6. For many applications, the temperature change can be considered instantaneous.

An ideal composite will have a Fickian diffusion where moisture absorption is time dependent [7]. The rate of moisture diffusion is known to be temperature dependent and can be described using an Arhenius equation (equation 9).

$$D = D_o \exp(-E_d / RT) \tag{6}$$

Where:

E_d = activation energy (cal/g-mol)
R = Universal gas constant (1.987 cal/g-mol-K)
T = absolute temperature (K)
D_o = Diffusion coefficient (cm^2/sec)

Moisture absorption of composites is influenced by many factors and is highly material dependent. In most cases, fiber diffusivity is negligible as compared to the matrix. Resins, such as epoxies, will absorb differently depending on their chemical structure. Typically vinyl ester resins will absorb less than epoxy resins [32].

Unfortunately, not all composites behave in a Fickian manor. Voids, cure shrinkage cracks, and other flaws may increase maximum moisture concentration as well as absorption rates [7]. Microcracks in composites allow for increased absorption due to

their capillary action. Stress levels will also change moisture absorption. Studies on composites by Gillat and Broutman [33] and later by Yaniv and Ishai [34] have shown higher diffusivity coefficients with increasing tensile stress levels. Yaniv and Ishai furthered the study showing decreased diffusivity with compressive stresses.

One can solve Fick's governing equation by setting boundary conditions where the concentration at the surface of the material (Cs) and the initial concentration of the bulk material (Co) are constants. Under the conditions of a replenished source the solution becomes.

$$\frac{C-Co}{Cs-Co}=1-erf[\frac{-x^2}{2\sqrt{Dt}}] \tag{7}$$

Where the Gausian error function (erf) is defined as:

$$erf(z)=\frac{2}{\sqrt{p}}\int_0^z e^{-y^2}dy \tag{8}$$

This method is very accurate for small times (i.e. initial stages of diffusion). Since error function tables have been created, numerical analysis is quite easy and quick. Fick's law can also be solved using the general equation:

$$c=\sum_{m=1}^{\infty}(A_m \sin l_m + B_m \cos l_m)e^{-l_m^2 Dt} \tag{9}$$

The solution becomes:

$$c(x,t)=\frac{4c_o}{\pi}\sum_{n=0}^{\infty}\frac{1}{(2n+1)}e^{-\frac{D(2n+1)^2\pi^2 t}{\ell^2}}\sin\left(\frac{(2n+1)\pi x}{\ell}\right) \tag{10}$$

Which can be expressed in terms of a percentage in the form,

$$\frac{c-c_i}{c_m-c_i}=1-\frac{4}{p}\sum_{n=0}^{\infty}\frac{1}{(2n+1)}e^{-\frac{D(2n+1)^2 p^2 t}{l^2}}\sin\left(\frac{(2n+1)px}{l}\right) \tag{11}$$

The total moisture weight can be calculated by integration

$$m=\int_0^l c\,dx \quad \Rightarrow \quad G\equiv\frac{m-m_i}{m_m-m_i}=1-\frac{8}{p^2}\sum_{n=1}^{\infty}\frac{e^{-\frac{(2n+1)^2 p^2 Dt}{l^2}}}{(2n+1)^2} \tag{12}$$

This solution is valid for all stages of diffusion. The disadvantage in calculation comes from the summation term. Mathematical models will be slow due to the large number of calculations summing from n=0 to infinity (or a large convergence value). Comparing experimental and analytical solutions from Fick's law can be seen in Figure 9. Notice that increasing the temperature increases both the maximum moisture content and the rate of diffusion.

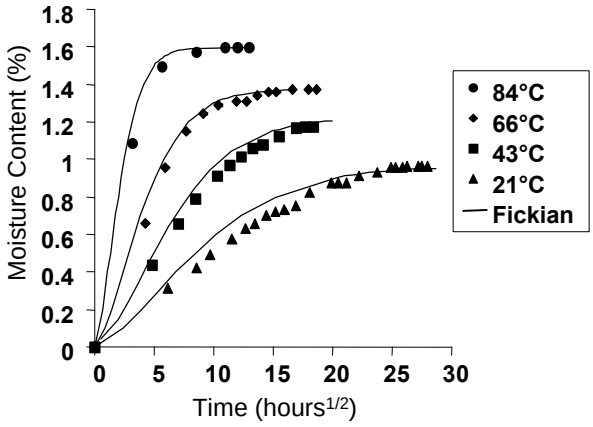

Figure 9. Comparison of experimental and Fickian diffusion. Results are for a vinyl ester/glass composite [35].

Not all composites will show Fickian diffusion. Cai and Weitsman [36] and Blikstad et al. [37] discovered two plateau regions. Cai and Weitsman described the depart from classical Fickian response as a viscoelastic mechanical response. Using Gibbs free energy methods, a time dependent diffusion process will be predicted. This time dependent phenomena will occur even under a constant ambient environment. Emri and Pavsek used the time-temperature superposition philosophy to describe diffusion as a time-humidity viscoelastic phenomenon [32]. Their model is based on the hypothesis that mechanical properties depend on the amount of free volume (intermolecular space), which in turn depends on the temperature, mechanical load, and quantity of diffused moisture. Blikstad et al. concludes that the first plateau is a function of the relative

humidity and residual stresses in the laminate. Compressive residual stresses will retard diffusion and lower the plateau levels. Yaniv and Ishai also studied the change in diffusion rate with load in polymeric adhesives [34]. They found that a tensile load increased diffusion rate while a compressive load decreased diffusion rate. Yaniv and Ishai found that low loads had a linear diffusion while higher loads had a non-linear diffusion.

2.3. Life Prediction: Cumulative Damage Models

Structures and machines are typically subjected to varying or random loads. For multi-stress loadings, the nature and prediction of damage state is more complicated than constant amplitude loading. For metals, simple models such as the Palmgren-Miner's Rule and Modified Palmgren-Miner's Rule were accurate. In metallic materials, fatigue damage is related to crack growth. Thus a simple life prediction model that uses a graduated deterioration due to cycles does work, regardless of the actual nature of damage.

In ceramics, composites, and concrete where fatigue deterioration cannot be easily described in terms of singe crack growth, variations of the Palmgren-Miner's Rule were inaccurate. In composite systems failure modes can occur from fiber-matrix debonding, fiber fracture, matrix failure, and delamination. These failure modes often form a nonlinear damage state when related to fatigue cycles. A damage model defined by these material property changes can be formulated as a function of number of cycles and applied stress level. That is, it often predicts lives greater than those observed through experiments. In these types of materials, damage progression is usually non-linear. The following subsections detail linear and non-linear cumulative damage laws used in metals and composite materials.

2.3.1. Palmgren-Miner's Rule

The most common damage law is the Palmgren-Miner's linear damage rule [38]. In this model, cumulative damage is linear with respect to the number of fatigue cycles,

and is independent of the value of the stress. This relationship (see equation 16) is defined by a parameter (d) and the ratio of fatigue cycles to the total number of cycles at the given stress level (n/N). The parameter, d, represents the fraction of catastrophic damage sustained after n cycles. Failure is defined when d = 1 and $n=N_f$. Thus, d also represents the fractional damage after cycling at a stress level, σ_i, for a fraction of life, n_i/N_i.

$$d = \frac{n}{N} \tag{13}$$

This model can be used to track life fraction (n/N) in multi-stress level fatigue situations. First convert equation 16 into a form that can be used in multi-stress fatigue analysis. Each block load segment, n_i, must have a known fatigue life, N_i. This load block then has its reduction in strength given as the ratio of n_i/N_i. The ratios for each load segment are then added and failure occurs when the summation of the $n_i/N_i = 1$ (see equation 17). Remaining strength can be tracked for any given number of cycles by simply subtracting the damage parameter from unity. For instance, in Figure 10 a three-step block load situation is shown. In the first step, a material is fatigued at a stress level where it would fail in 100,000 cycles for only 40,000 cycles. This reduces the life by a ratio 40,000/100,000, thus only 60% of the original strength is left. The next step changes the stress level to where fatigue life would fail in 25,000 cycles. This is cycled for 10,000 cycles and another 40% reduction in strength. Thus the total reduction is .4 + .4 = .8. The final step returns the load back to one that would fail in 100,000 cycles and fatigues until failure. Using this model, failure would occur in 20,000 cycles, which is 20% of 100,000.

$$d = \sum \frac{n_i}{N_i} \tag{14}$$

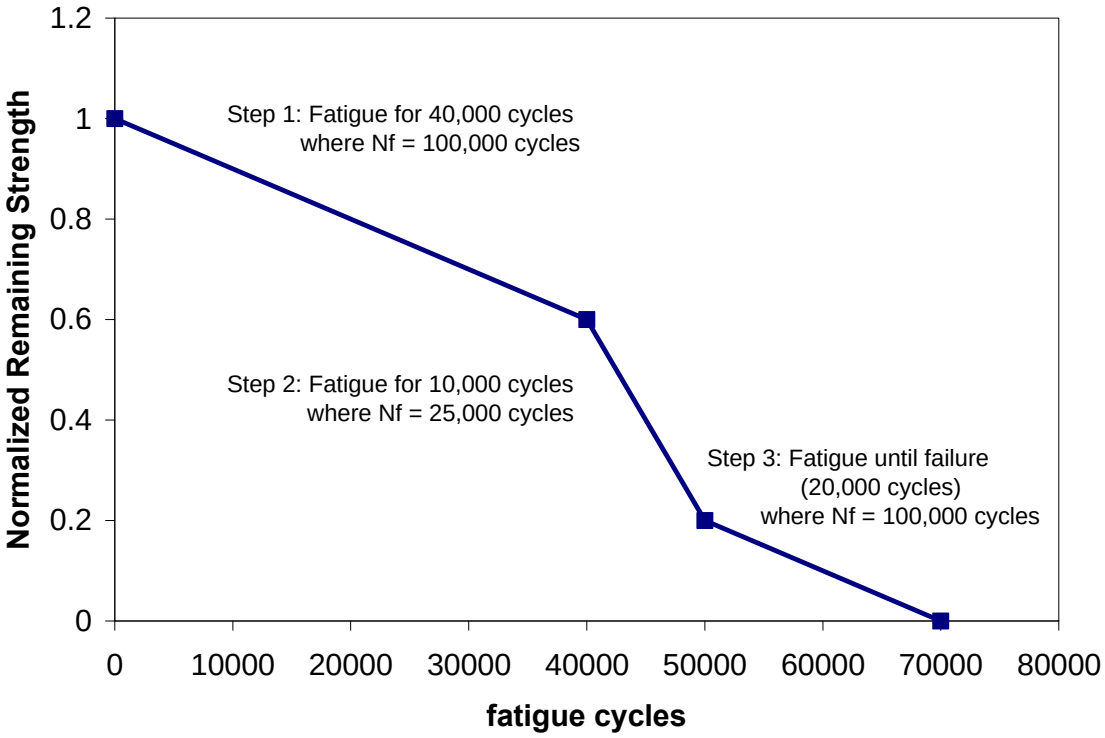

Figure 10. Schematic showing Palmgren-Miner's linear damage accumulation model.

Although the Palmgren-Miner's rule is not an accurate life prediction method of composite materials, due to its simple calculations, is often used to compare data. Adam et al. [39,[40] used the Palmgren-Miner's rule to begin the study of a non-linear damage model. Adam et al. looked at the response of a repeated unit of four different load levels to an aerospace composite material. For tension-tension-tension-tension (TTTT) type of block loading it was shown that a lower initial stress appears to be more beneficial to the lifetime than a higher initial stress. Another result was that large changes in load size caused more harm than smaller changes in load. Nearly all failures occurred during the largest load cycles. Adam et. al then used these results to create a power law for fractional damage in terms of fractional life, with the damage index in the power law to be stress dependent. The model increased the accuracy of the predictions for all the different loading schemes mentioned.

2.3.2. Modified Palmgren-Miner's Rule

The simplest step forward from the linear damage rule is to look for non-linear functions that still employ the damage parameter, d. One method is the Modified Palmgren-Miner's Rule. This method uses the base form and includes a shape parameter, α, which is a function of the stress amplitude (see equation 18). The shape parameter is found empirically and is independent of applied stress level. Failure still occurs when d = 1.0. The difference between the Pamlgren-Miner's and Modified Palmgren Miner's Rule is shown schematically in Figure 11. In this schematic, the shape parameter is given a value of 2. It is easy to see that different numbers of cycles are necessary to achieve equivalent fractional damage.

$$d = \left(\frac{n}{N}\right)^{a} \tag{15}$$

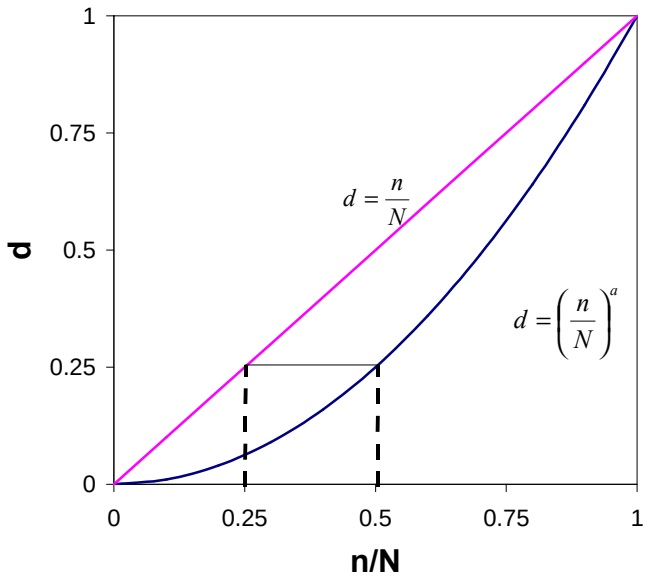

Figure 11. Schematic illustration of linear and non-linear damage accumulation models. Note that different numbers of cycles are necessary to reach equivalent fractional damage amounts.

Alessandro Zago, George Springer and Marino Quaresimin [41] used the modified Miner's rule to estimate fatigue life of short fiber reinforced thermoplastic

parts. Test coupons were fatigued for two level block loads for various load schemes. Fiber volumes of 30% and 50% were used. The data was then used to determine an α that best fit the data. For the short glass fiber reinforced copolyamide, αs ranged from 0.90 to 0.95 with an average value of 0.92. In another study by Zago and Springer [42], fatigue lives of short fiber reinforced thermoplastic automotive gear shift links were estimated using the modified Miner's rule and data from fatigue testing of coupons with holes.

The Modified Palmgren-Miner's Rule was also a good tool in predicting life for metallic components. Marco-Starkey [43] later expanded the Modified Palmgren-Miner's rule by presenting a model in which a is stress level dependent (equation 19). Thus, the shape parameter for each applied stress level must be determined experimentally.

$$d = \left(\frac{n}{N}\right)^{a_i}, \qquad \alpha_i > 1 \tag{16}$$

Evaluation of this model with applied stress level shows a condition seen schematically in Figure 12. For increasing stress level, where:

$$r_1 > r_2 > r_3 \tag{17}$$

It can be seen that the shape parameters follow the trend where:

$$1 < \alpha_1 < \alpha_2 < \alpha_3 \tag{18}$$

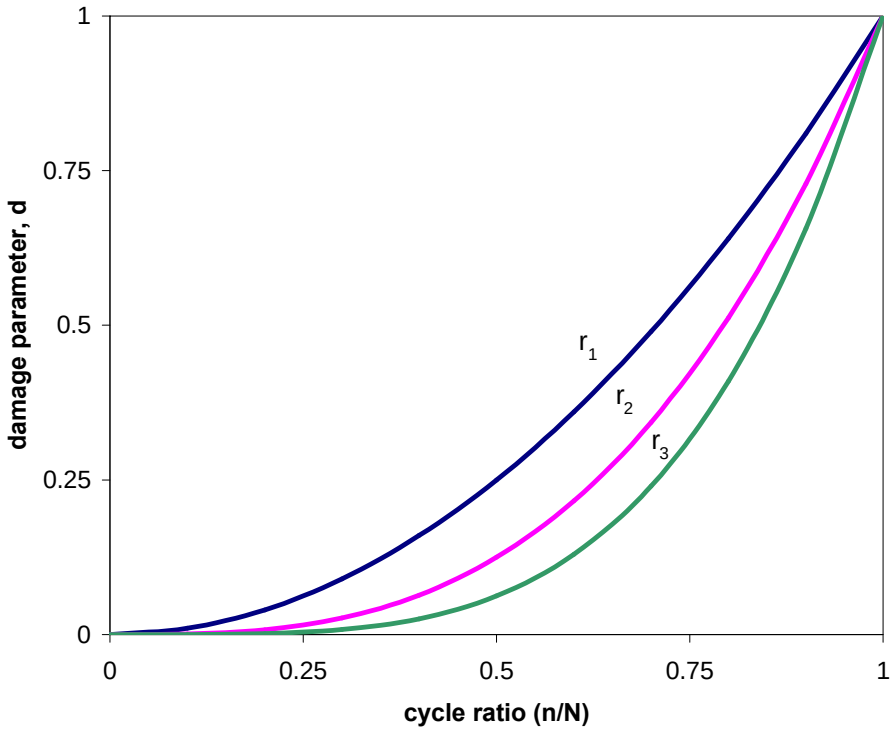

Figure 12. Marco-Starkey's damage parameter as a function of applied stress level.

2.3.3. Remaining Strength Models

Broutman and Sahu [44] developed a linear model that tracks life fraction (see equation 22). The element S_r/S_{ult} is also described as the remaining strength function, or F_r, where a value of 1.0 is considered undamaged. The term S_a/S_{ult} is defined as the failure function, or F_a. Failure is said to occur when the applied load equals the remaining strength of the material, or when $F_a = F_r$.

$$\frac{S_r}{S_{ult}} = 1 - \left(1 - \frac{S_a}{S_{ult}}\right)\frac{n}{N} \tag{19}$$

Reifsnider and Stinchcomb [45] extended this model by adding a shape parameter,j, to the Broutman and Sahu equation. Just as seen in the Modified Palmgren-Miner's rule, the j value is determined experimentally.

$$\frac{S_r}{S_{ult}} = 1 - \left(1 - \frac{S_a}{S_{ult}}\right)\left(\frac{n}{N}\right)^j \tag{20}$$

Comparison of j values can be seen in Figure 13. A j value greater than 1 shows a convex curve and indicates catastrophic failure. Unidirectional carbon fiber composites show catastrophic failure and typically have j values around 1.3. A j value less than 1 indicates rapid initial decrease in strength. A j value of 1.0 gives the Broutman-Sahu expression with a linear reduction in remaining strength. Glass fiber composites typically have j values around .95 to 1.0.

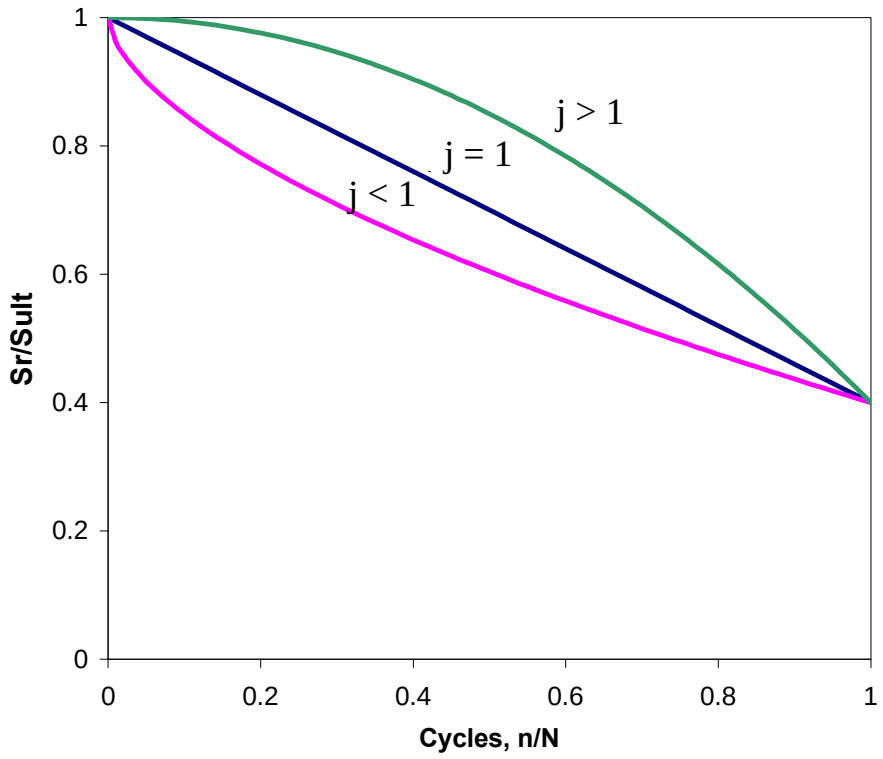

Figure 13. Remaining Strength curve comparing j values.

2.3.4. Remaining Strength Model Utilizing the Critical Element Model

As stated earlier, composite failure modes include fiber-matrix debonding, fiber fracture, matrix failure, and delamination. One method of using the Reifsnider-Stinchcomb model is to define the failure mechanism. The Critical Element Model makes use of a representative volume element (RVE) as in continuum mechanics. The RVE is sufficiently large to describe the damage state. For example, consider a composite with 0° fibers. Fiber failure could be described when enough adjacent fibers fail (see Figure 14). Thus, global failure can be explained using a local failure criterion.

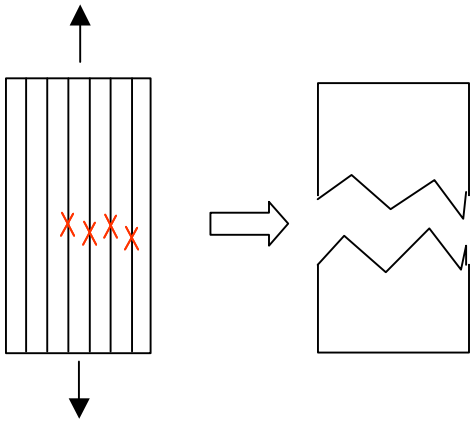

Figure 14. Critical element model basing failure upon 0° fiber failure.

In this case the failure function, designated Fa, is based upon the maximum tensile strength of the material, Xt, and the axial stress in the 0° fibers, $\sigma_1^{0^\circ}$ (see equation 24). Other ply orientations are then defined as sub-critical elements and control the stress state of the material. For instance, it is known that during fatigue of cross-ply laminates matrix cracks develop in the off-axis plies. Since less load is transvered to these plies this damage in turn increases the stress in the critical 0° fibers.

$$Fa = \left| \frac{s_1^{0^\circ}}{Xt} \right| \tag{21}$$

The power in the critical element model is the accuracy achieved in multi-stress fatigue life predictions. The best way to explain this is using an example of a two-step load pattern as shown schematically in Figure 15. This schematic shows a situation where a constant amplitude stress is applied for a finite number of cycles. The amplitude and mean stress are then decreased and the material is fatigued until failure. Using equation 25, the remaining strength can be calculated for the first block load step (see Figure 15). Using the concept of pseudo-cycles, this can then be traced to an equivalent remaining strength point on a remaining strength curve for the next load level. The pseudo-cycles represent the number of cycles, from the second load level, which would create an equivalent remaining strength. This is calculated from the system of two equations, which simply sets S_a/S_{ult} (from equation 25) to equal F_{a1} and F_{a2}, and S_r/S_{ult} equal to F_{r1} and F_{r2}.

$$\begin{aligned} Fr_1 &= 1-(1-Fa_1)\left(\frac{n_1}{N_1}\right)^j \\ Fr_2 &= 1-(1-Fa_2)\left(\frac{n_2{}^o}{N_2}\right)^j \end{aligned} \tag{22}$$

By setting Fr_1 equal to Fr_2 and solving for the pseudo-cycles, $n_2{}^o$ one obtains:

$$n_2{}^o = \left(\frac{1-Fr_1}{1-Fa_2}\right)^{\frac{1}{j}} N_2 \tag{23}$$

Remaining strength for the second load step is then started from the pseudo-cycle initial point and can then be calculated for the remainder of the fatigue life. For multi-

stress loading with many block loading steps, this calculation can become quite tedious. By rewriting our evolution expression for Fr in the form of equation 27 and integrating, we may obtain with an equation that is better suited for handling many multi-stress conditions.

$$\frac{dF_r}{dn} = -(1 - F_a) j \frac{1}{N} \left(\frac{n}{N} \right)^{j-1}$$
$$Fr = 1 - \left\{ \int_0^n (1 - Fa)^{1/j} \frac{dn}{N} \right\}^j \qquad (24)$$

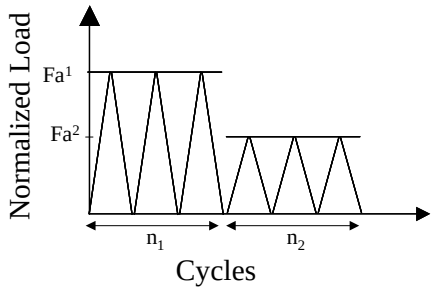

Figure 15. Schematic showing multi-stress load example for introduction of psuedo-cycles concept.

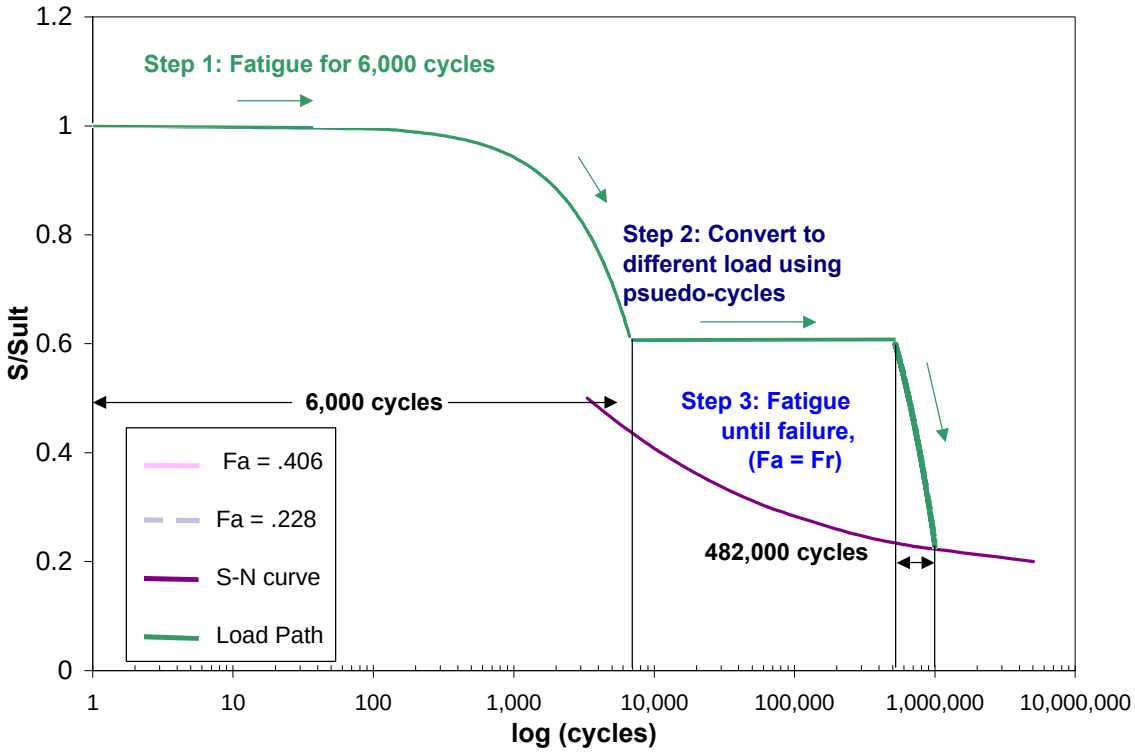

Figure 16. Schematic showing remaining strength path for a multi-load scenario.

Chapter 3. Materials and Experimental Methods

3.1. Materials

The material used in this investigation is a vinyl ester/E-glass composite manufactured using the continuous resin transfer molding technique (outlined in the literature review). The matrix is Dow Chemical's Derakane 441-400 vinyl-ester modified epoxy resin. To aid in the CRTM process, resin viscosity was reduced by the addition of 28% by resin volume of styrene. During a pultrusion process, a 6% shrinkage was seen in the pure resin. This is higher than is seen in epoxies. The glass fiber is PPG Hybon 2002 E-glass.

Table 1. Matrix, Fiber, and Composite Properties

	Tensile Strength	Tensile Modulus	Elongation
Material	(psi)	(Msi)	%
Derakane 441-400	13000	0.52	7.50
PPG Hybon 2002 E-glass	246500	11.02	3.10
$(0/90/(\pm45)_2/0/90)_{2T}$ Composite	37065	2.80	2.00

The lay-up is $(0/90/(\pm45)_2/0/90)_{2T}$. This laminate is very close to being a symmetric quasi-isotropic laminate, except that the ±45 layers alter the symmetry. Thus, this laminate must be called non-symmetric. The volumetric ratio of the 0°, 90°, and ±45° laminates is 2/3/2.5, therefore the laminate is unbalanced as well.

The fibers were arranged and stitched, by a non-crimped fabric (NCF) stitch process, to aid in the pultrusion process. The stitch was arranged at 7 stitches per inch transverse to the stitch direction and a penetration along the length of stitching direction of approximately 1/10 inch. The stitch composed only 1% of the glass fiber weight. A tricot stitch was used for the 0/90 plies, while a chain stitch was used for the ±45 layers

(see Figure 17). The tricot stitch consists of zigzag stitch loops around the 0° and 90° fiber bundles. These zigzag stitches pass around an axially aligned carrier thread. This stitch process creates a gap between the fiber bundles, creating a resin rich region. This region will be discussed in more detail later.

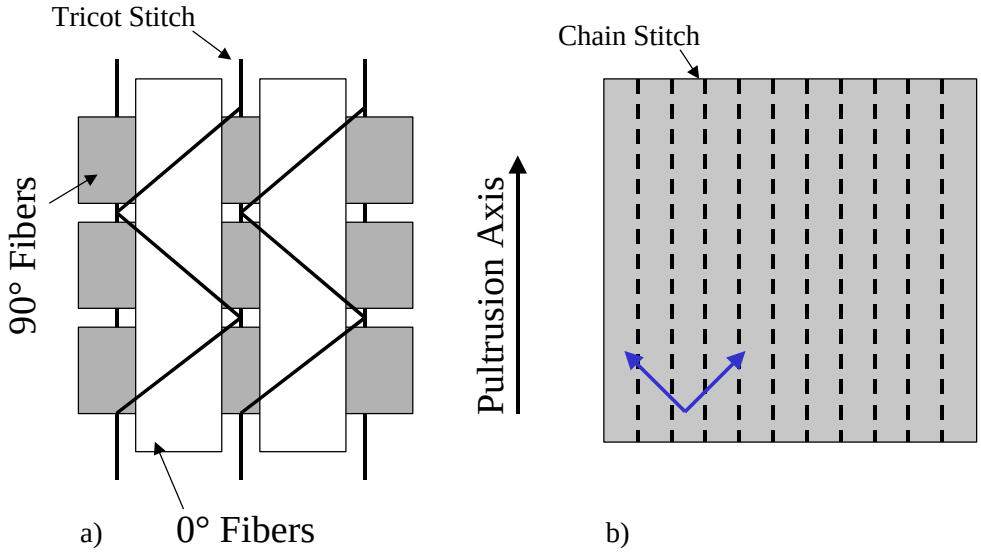

Figure 17. a) Tricot stitch geometry. Notice the gaps that will allow resin rich regions. b) Chain stitch pattern.

The CRTM pultrusion process created a variety of imperfections within the composite including local fiber volume variations, warp of the specimen, pure resin rich regions, non-uniform surface, microcracking, delaminations, voids and fiber undulation. The local fiber volume variation is a direct function of the stitched fiber geometry, since the stitching separates the fiber tows. Matrix shrinkage created a textured surface and internal microcracking. The lay-up of the fibers also created fiber undulation, local fiber volume variation, and resin rich region problems. The tricot stitch from the non-woven fabric forced the fabric into a non-uniform fiber pattern. This was seen in both the axial and transverse to pultrusion directions. The axial, or 0°, fiber bundles were gathered by the tricot stitch into a bundle, creating gaps between axial fiber bundles.

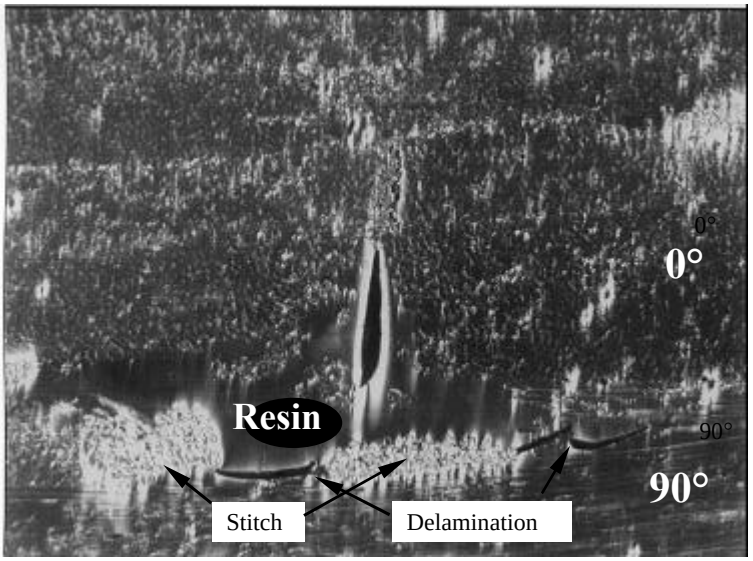

Figure 18. Micrograph of $(0/90/(\pm 45)_2/0/90)_{2T}$ laminate showing a resin rich region, a delamination, and stitching. (photo courtesy of S. Phifer [24])

The 0° fiber bundles can create one of two geometries; a nested or aligned pattern (Figure 19 and Figure 20). The nested fiber alignment creates a large fiber undulation problem in the transverse 90° plies, and only a slight fiber undulation in the 0° plies. During tension, these undulated fibers will want to align with the load. Although the axial modulus will increase, microcracks may form. The aligned configuration has less fiber undulation, but creates a larger resin rich region. Since there is not an applied tensile force in the transverse direction during processing, the 90° fibers will bulge in the direction of the resin rich region. During curing, the resin rich region will undergo matrix shrinkage, which can create microcracking.

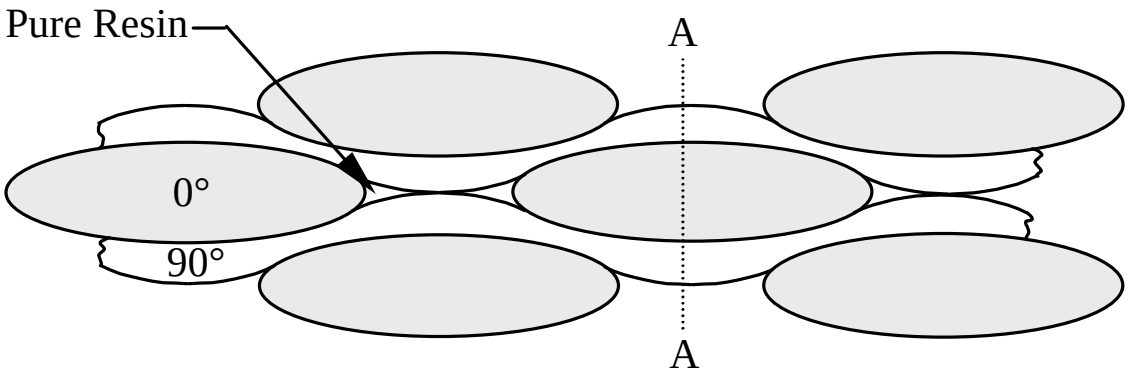

Figure 19. Nested fiber geometry. The adjacent 0° fiber bundles of the non-woven stitched fabric creates a high fiber undulation in the 90° plies (photo courtesy of S. Phifer [24])

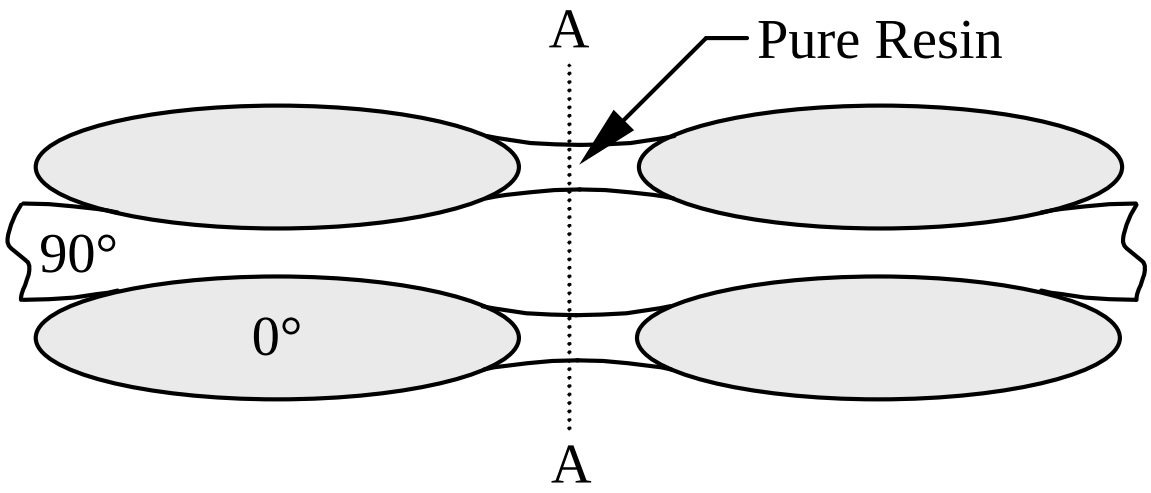

Figure 20. Aligned fiber geometry. The stitching separates the 0° fiber bundles in such a way that creates a resin rich region (photo courtesy of S. Phifer [24])

Other researchers using various cure cycles have studied Derakane 441-400 vinyl ester resin cured with 1.1% of low temperature initiator, Benzoyl Peroxide (BPO), and 28% styrene. Specimens using the exact CRTM pultrusion process cure cycle were

impossible to create since high cure shrinkage caused complete fracture. The pultrusion process cure cycle is 5 minutes at 150°C in a heated die. The cure profile that was most similar to the pultrusion process and didn't fracture was a ramp from 20° to 150° C at 6.5° C per minute, followed by a 20 minute hold at 150 and a –2° C per minute ramp to room temperature. The tensile strength and modulus of these specimens were 8 ksi and .5 Msi respectively. The failure strain was 1.9 % (in/in). These compare well to Dow Chemical technical data sheets of Derakane 441-400. The tensile strength, modulus and failure strain given by Dow are 13 ksi, .52 Msi, and 7% elongation. Note that Dow's material does not have the increased styrene content, thus material property differences are expected.

3.2. Quasi-Static Evaluation of Vinyl Ester/E-glass Composites

The material system in this investigation has already received extensive analysis by Steven Phifer [24]. Phifer performed quasi-static and fatigue evaluation on different types of laminates of vinyl ester/E-glass composite. The $(0/90/(\pm 45)_2/0/90)_{2T}$ quasi-isotropic laminate used in my investigation is, in fact, surplus material from Phifer. The micrograph in Figure 21 shows resin rich regions and the fiber geometry for the quasi-isotropic laminate. This section will outline the quasi-static evaluation of this laminate, denoted QI1.

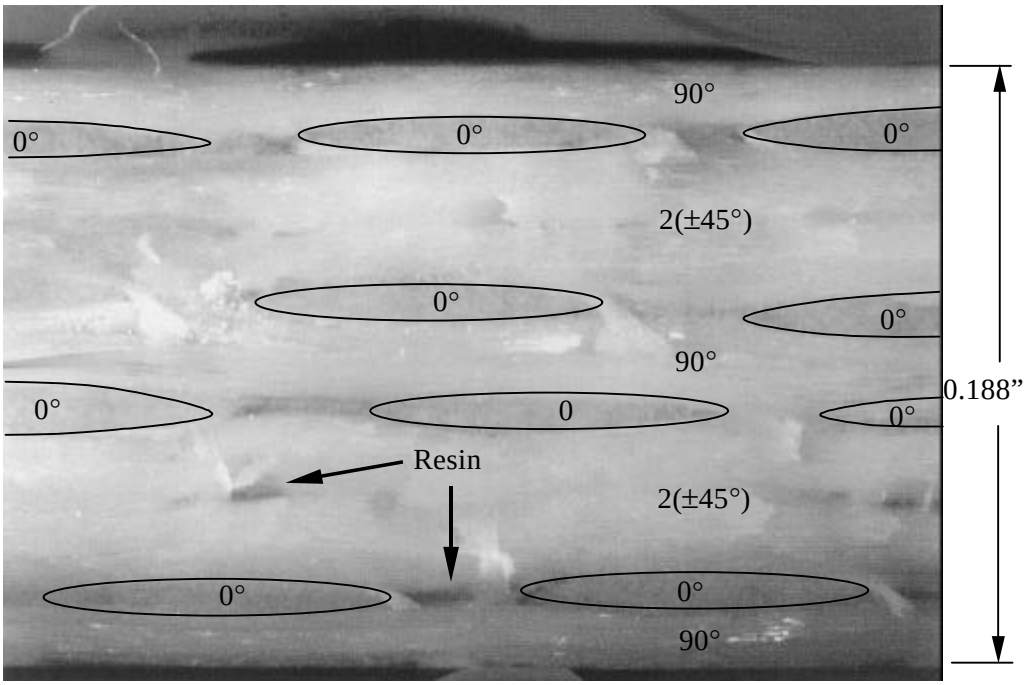

Figure 21. Micrograph of $(0/90/(^{+}_{-}45)_2/0/90)_{2T}$ laminate. The view is of a cross section that has been cut perpendicular to the pultrusion direction. Thus, the 0° fibers are pointing out of the page. (photo courtesy of S. Phifer [24])

Neat resin and unidirectional composites were quasi-statically tensile tested to determine ply properties for the quasi-isotropic laminate. Ply properties will be based on these results but, due to the woven geometry of the pultruded composite, they will be slightly different. The extraction method of ply level properties is discussed by Phifer

[24]. The results are tabulated in Table 2. These values will be used later in the computer simulation and life prediction. Ply strength will be based off of the 111.9 ksi value given by Phifer.

Table 2. Ply level properties for quasi-isotropic laminate of vinyl ester/E-glass composite.

Designation	Ply Orientation	Vf % Fiber Volume	Modulus (Msi)	Ultimate Tensile Strength (ksi)
Matrix	none	none	0.499	8
Unidirectional	0°	71%	7.467	142.8
QI1	$(0/90/(\pm45)_2/0/90)_{2T}$	56%	2.8	34.8
QI1(ply properties*)	-	56%	5.6	111.9

* ply properties extracted from quasi-isotropic laminate. Procedure is described by Phifer [24].

3.3. Fatigue Evaluation of Vinyl Ester/E-glass Composites

Fatigue testing of the QI1 laminate determined S-N curves and remaining strength curves was completed by Phifer [24]. Testing was done using a servo-hydraulic MTS test frame under load control. Fatigue cycling was completed at a frequency of 10 Hz and an R ratio of 0.1. The results of this section will be used in the computer simulation and life prediction.

S-N curves varied with each laminate. The slope of the curve tended to decrease with decreasing stress level. The slope for the QI1 quasi-isotropic laminate, between a normalized tensile stress of .3 and .2, is approximately 10% per decade. This is quite comparable with literature data. Mandell conducted fatigue test on a variety of short and continuous glass fiber composites with an assortment of matrices. He discovered that the glass fiber dominated the failure and for all glass fiber composite the normalized S-N curve had a slope of 10-11 percent per decade. Mandell postulated that glass fiber fatigue tensile strength is dominated by fiber properties [25], [26].

The S-N curves for this laminate are lower than that for the literature values. This drop is due to the fiber geometry and processing of the composite. In these tests, the tricot stitch of the non-woven non-crimped fabric gathered the axial fiber bundles, creating fiber undulation in both the axial and transverse direction to the pultrusion axis.

This fiber geometry causes defects including fiber waviness, stitch stress risers, microcracking and slight delamination in the as-processed state.

The S-N curve can be modeled using an exponential equation. For the quasi-isotropic laminate, the equation takes the form of:

$$Fa = a - b \bullet (Exp(-c * n / N)^d) \qquad (25)$$

where:

a = .9999763

b = .82678917

c = 10.29539

d = -.3721723

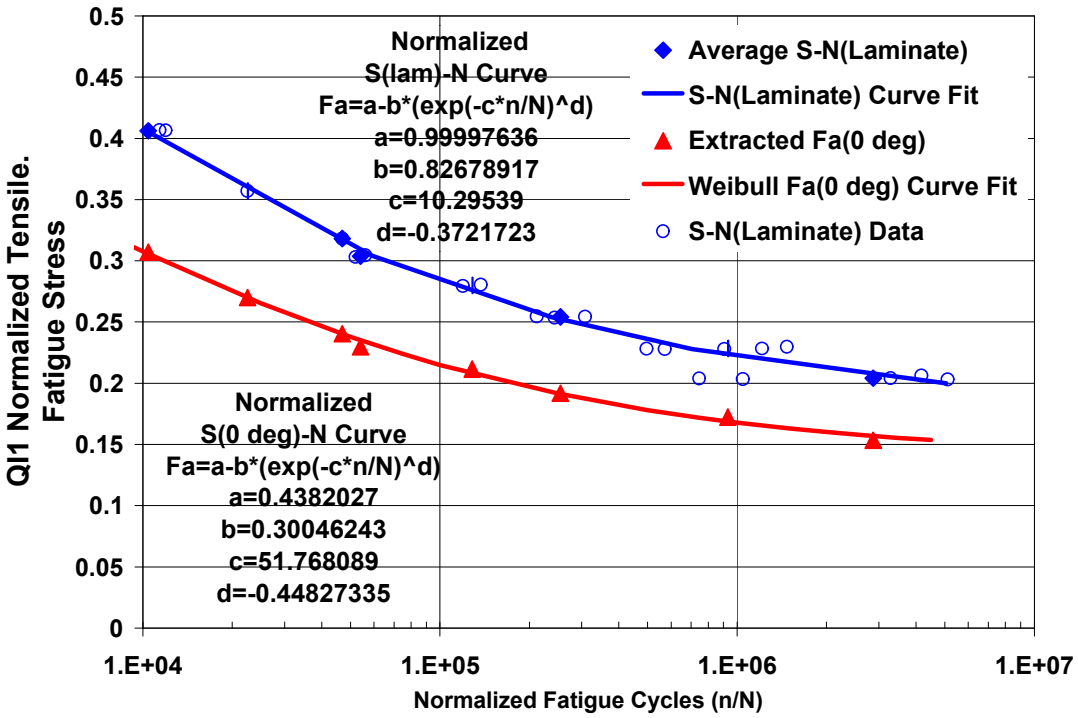

Figure 22. Normalized Axial Tensile Fatigue Stress vs. Failure Cycles for QI1 Laminate: Measured Laminate & Extracted Critical Element (0° plies) [24].

3.3.1. Off-axis Stiffness Reduction

Stiffness reduction due to transverse cracking in composite laminates is not a new concept and has been studied since the early 1970s. The first work to associate stiffness degradation with transverse cracking was Hahn and Tsai [46]. During uniaxial loading of cross-ply laminates, cracking is assumed to occur in the 90° plies. This cracking creates a local reduction in cross-sectional area. Derived expressions netted a bilinear stress-strain relationship in which the onset of transverse cracking decreased the effective modulus of the laminate. This type of behavior is indicative of experimental data.

Reifsnider, et al [47] furthered transverse cracking research while investigating multidirectional laminates. Reifsnider et al. discovered the existence of a crack pattern that developed during sufficient loadings and is described as a Characteristic Damage State (CDS). The loads that developed CDS was either a high monotonic load or from a sufficient number of cycles of lower load. The CDS consisted of nearly uniform spacings between cracks in individual off-axis plies. The crack spacings were found to depend on the laminate configuration. Reifsnider [48] showed that this distinctive crack pattern could be predicted by a shear lag analysis.

In this analysis, stiffness reduction of the composite was modeled using an empirical formula based on experimental data [24]. Stiffness reduction curves were determined from fatigue data (see Figure 23). An extensometer was used to determine the laminate stiffness during fatigue testing. Only off-axis stiffness was assumed to reduce as a function of fatigue cycles. This is assumed to happen in the form of matrix cracks. The 0° fibers were assumed to have no stiffness reduction.

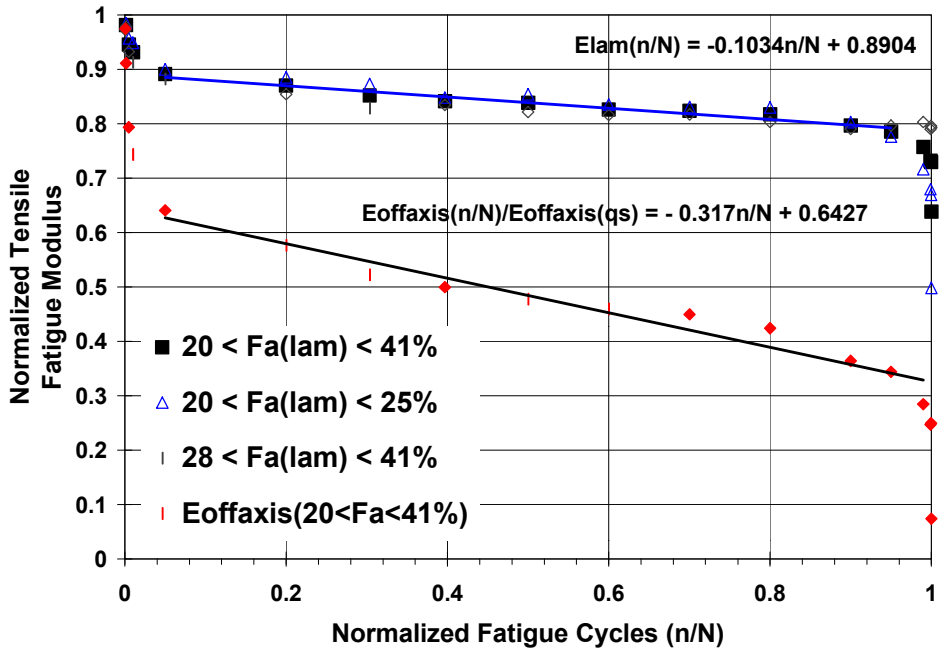

Figure 23. Normalized Tensile Fatigue Off-Axis Modulus Reduction for QI1. (Data courtesy of S. Phifer [3]).

Results determined the reduction in off-axis stiffness as a function of fatigue loads, modeled using a linear trend line, to give the equation:

$$\frac{E_2(n)}{E_2(q.s.)} = -.317\left(\frac{n}{N}\right) + .6427 \tag{26}$$

Where $E_2(n)$ and $E_2(q.s.)$ are the off axis modulus at a given fatigue cycle and from quasi-static data respectively. The data for this is shown in Figure 49.

The laminate modulus shows three distinct regions. The first region occurs within the first 5% of its life and drops as much as 18% of its ultimate tensile strength. The next region shows very small changes in modulus. Within the last 10% of the lifetime, the modulus decreases rapidly as fibers begin to fail.

3.3.2. Remaining Strength

Remaining strength can be calculated by fatiguing specimens at various load levels for different numbers of cycles (equation 3). The fatiguing is then followed by quasi-static tensile tests to determine the residual strength. Using this expression, the j factor was determined to be .95 for the vinyl ester/E-glass composite.

$$Fr = 1 - (1 - Fa)(n / N)^{j} \tag{27}$$

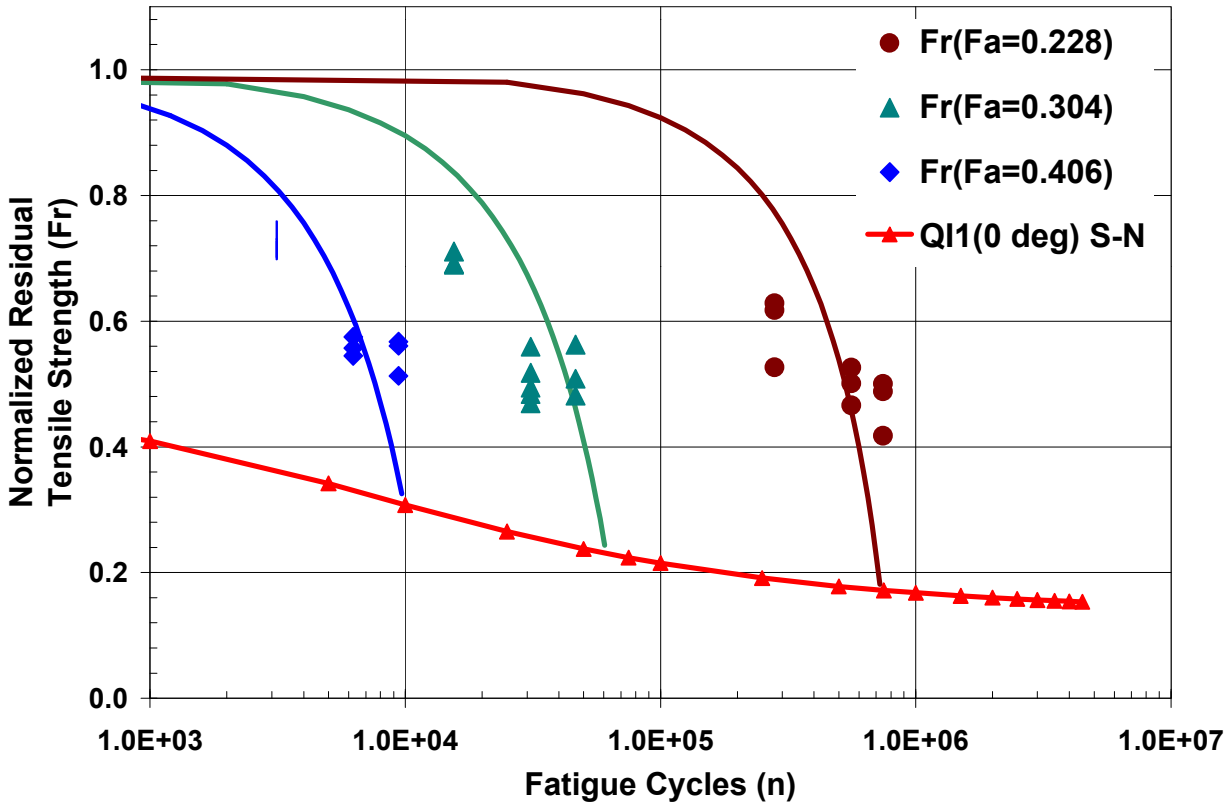

Figure 24. Remaining Strength Correlation for QI1 Using S-N, X_i, E_i, & Stiffness Reduction from QI1 Laminate. (Data courtesy of S. Phifer [3]).

3.4. Specimen Preparation

3.4.1. Tensile Specimens

Composite panels measuring 6” (15.24 cm) wide, .186” (.472 cm) thick, and approximately 6 feet (2 meters) long were cut using a wet diamond saw to 1” (2.54 cm) by 7” (17.78 cm) long. The edges of the specimens were ground with 240 and 400 grit sandpaper to remove diamond saw blade marks. The specimens were then measured with calipers to determine cross sectional area. A two-part epoxy was then used to seal the edges and to inhibit moisture absorption through the edges. The two- part epoxy was cured at room temperature for twenty-four hours, followed by a two hour post cure at 55° C. This procedure was done on all specimens throughout this study. Even specimens used in the elevated temperature studies, where moisture absorption was not an issue, had edge coating.

3.4.2. Specimen Preparation for Aging Bath

The composites were aged at 95°, 113°, 131°, and 149° F (35°, 45°, 55°, and 65° C) in a water bath. These temperatures were chosen in order to stay far enough below the glass transition temperature, 296.6°F (147° C) from DMA studies, such that the morphology of the resin would not change. The aging bath consisted of a 20-gallon polypropylene tank (See Figure 25). The tank was insulated with two inches of Styrofoam insulation and placed in a ¾ inch plywood box. Four fully submersible aquarium heaters (150 Watt by Whisper Inc.) were placed at each corner of the tank, and were controlled by an Omega controller. An aquarium pump (PowerHead 402 type made by Hagen), was placed at one end of the tank to circulate the water and insure uniform heat distribution. Specimens were arranged in plexi-glass racks, to ensure sufficient and

equal access to moisture on all sides (although the schematic in Figure 25 shows only one rack, two were used).

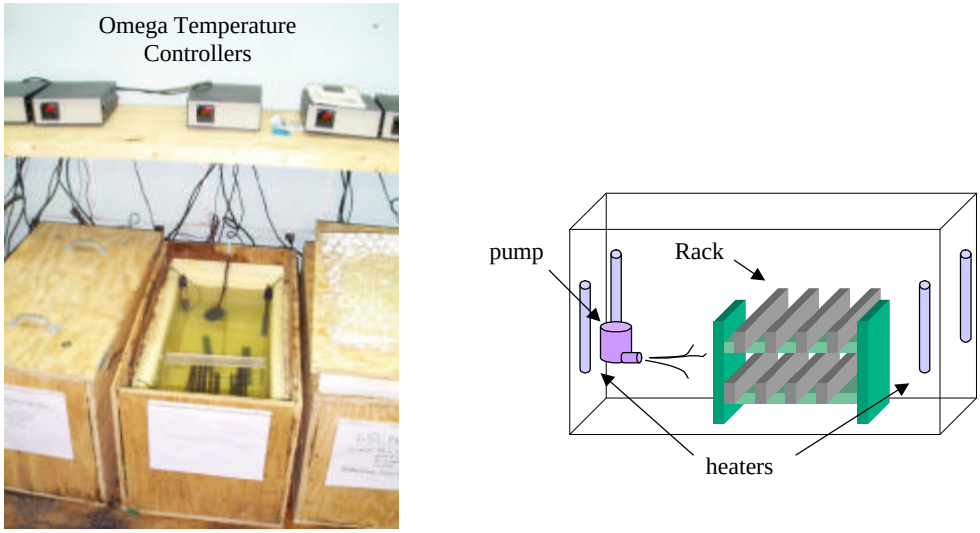

Figure 25. Picture and schematic showing location of the aging bath, heaters, pump, and specimen rack. The temperature is held constant using an Omega temperature controller.

Specimens were weighed before and after aging in order to determine moisture uptake. Moisture uptake monitoring was done regularly. The specimens were taken out of the tank and set into a cold bucket of water in order to slow outward diffusion of water during the moisture reading. The specimens were then wiped dry and placed on a Mettler AE 200 balance. The percent moisture uptake was measured using the following equation.

$$\%M = \frac{Wx - Wo}{Wo} \qquad (28)$$

Where:

Wx = wet weight at time x

Wo = dry weight at a time of 0

%M = percent moisture uptake

3.4.3. Determination of Diffusion Constant and Activation Energy

Moisture diffusion, as shown by the Arrhenius equation, is temperature dependent. Higher temperatures will have increased rates of diffusion as well as higher levels of moisture saturation. The rate of diffusion can be determined experimentally by conducting moisture uptake studies at a range of temperatures. To begin this, lets recall the Arrhenius equation.

$$D = D_o \exp(-E_d / RT) \tag{29}$$

where E_d, D_o, R, and T are the activation energy, diffusion constant coefficient, universal gas constant, and temperature in degrees Kelvin respectively. This equation can then be reduced to a linear form by taking the natural log of both sides of the equation.

$$\ln(D) = \ln(D_o) - \left(\frac{E_d}{R}\right)\frac{1}{T} \tag{30}$$

Using the initial slope of the moisture curve, the diffusion coefficient for a particular temperature can be calculated from:

$$D = \left(\frac{\ell\sqrt{p}}{4M_m}\right)^2\left(\frac{M_2 - M_1}{\sqrt{t_2} - \sqrt{t_1}}\right)^2 \tag{31}$$

where l, and M_m are the thickness, and maximum moisture (plateau of the curve). By using the values for D from equation 31, the diffusion constant coefficient (Do) and activation energy (Ed) can be calculated from the intercept and the slope of a ln(D) vs. 1/T plot.

3.4.4. Specimen Preparation for Aged Fatigue Testing

Fatigue testing was done on aged specimens. A transparent fluid cell was designed to keep the gage section of the test coupon in constant contact with water. The cell has a central depression where the fluid is circulated through (see Figure 26).

Silicone adhesive (General Electric^{TM} RTV 201) is used to seal the specimen in the fluid cell, while nuts and bolts are used to keep a tight seal. After application of the adhesive, the specimen and fluid cell are sealed in a zip-lock bag and stored in a refrigerator to reduce outward diffusion. Moisture tests showed that the combination of zip lock bag and refrigerator yielded less that .01% change in moisture after thirty days. Since the specimens are tested within a few days of preparation, moisture loss is assumed to be negligible. The fluid cell does not leak during cycling. Leaks may occur upon failure of a specimen.

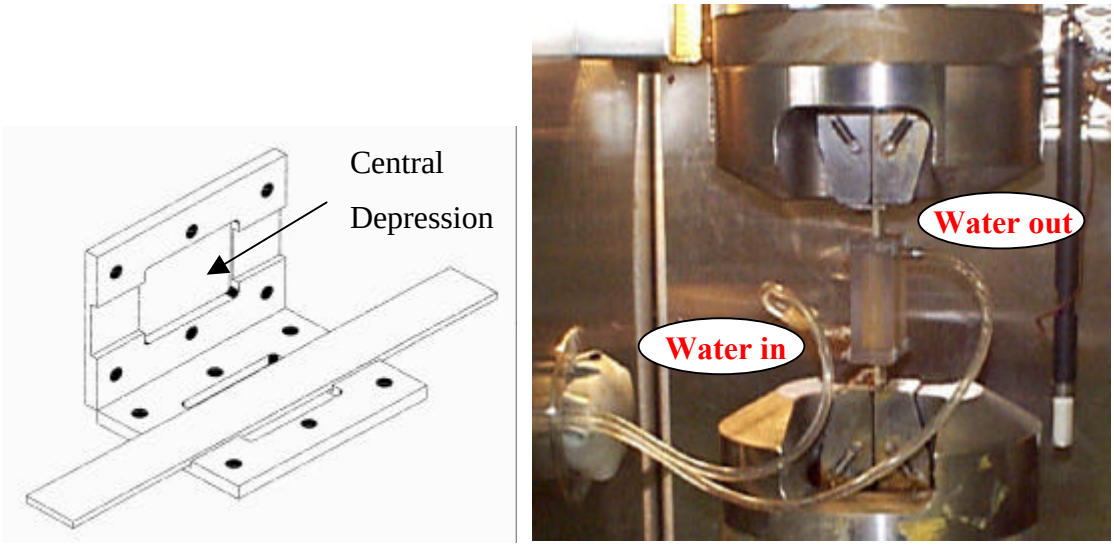

Figure 26. Fluid cell used for tensile testing of composite specimens. Water fills the central depression, keeping the specimen in constant contact with water while regulating temperature.

3.5. Experimental Methods

Various laboratory experiments were exercised to determine the response of the vinyl ester/E-glass composite to moisture, temperature and fatigue testing. The following subsections detail the experimental methods for each of these areas.

3.5.1. The Affects of Moisture on Vinyl Ester/E-glass Composites

Three different types of moisture studies were done. Moisture uptake studies were done to find the maximum moisture, diffusion constant, and activation energy. Strength as a function of moisture content and aging temperature were investigated from data collected from quasi-static tension tests at 0.60% relative moisture content. Finally, an S-N curve was created from fatigue tests at 0.60% relative moisture content. This subsection will detail the experimental methods used in these three studies.

Moisture uptake tests were done at 95°, 113°, 131°, and 149° F (35°, 45°, 55°, and 65° C). By studying the moisture uptake as function of temperature, the diffusion constant and activation energy can be obtained. These constants will be used later in the simulation to predict moisture content. Tensile tests were also done at different levels of moisture content. Target relative moisture contents are 0.15, 0.30, 0.45, and 0.60 % moisture. Tensile testing was then done at room temperature on an Instron displacement controlled test frame. Another test studied the effect of aging time on tensile tests. Specimens were aged at 95°, 113°, 131°, and 149° F until 0.30% relative moisture was achieved. Quasi-static tensile testing at room temperature then followed aging. Since it will take longer for the cooler temperatures to reach 0.30% moisture content, the composites will be in contact with the water for a longer period of time. This investigation will determine if a longer period of time has an effect on tensile properties.

The effect of moisture on fatigue properties was determined by creating an S-N curve. Composites were aged at 149° F until 0.60% moisture content was reached. Testing was done using an MTS servo-hydraulic test frame in load control. A fluid cell (see Figure 26) was used to keep the gage section of the specimen in constant contact with water, thus eliminating outward diffusion of water during the test. A water circulator kept the water at a constant 86° F (30° C) temperature. The test was completed inside an environmental chamber, where the temperature was dropped to 0° F. Dropping the temperature outside the gage section increased the tensile strength of the composite, thus creating a temperature stress concentration. Failures were then constrained to the

gage section. Stress levels used in this study ranged from 35 to 60% of ultimate tensile strength.

3.5.2. The Affects of Temperature on Vinyl Ester/E-glass composites

Quasi-static tensile tests were done at 0°, 25°, 50°, 75°, and 100° F (-17.8°, -3.8°, 10°, 23.9°, and 37.8° C). These temperatures represent a wider range of temperatures than that seen at the Tom's Creek Bridge (temperature, measured over the 1998 year at the bridge, ranged from 8° to 92° F). Tensile tests were done using a servo-hydraulic MTS load frame under load control. A ramp rate of 80 pounds per second was used. Strain gages were used to monitor displacement and modulus calculations. Specimen dimensions measured 1 inch wide, 0.186 inch thick and 7 inches long.

3.5.3. Cyclic Temperature Testing

Haramis [23] determined that cyclic temperature causes a reduction in strength of a composite material. A changing internal stress state, which results from the changing temperature, may cause this reduction in strength. Haramis developed a four point bend apparatus that applied a constant strain on a specimen. Specimens were put into the apparatus and placed in an environmental chamber where the temperature was cycled between 0° and 86° F (–17.8° and 30° C). Specimens were also placed in the environmental chamber in racks without a bending load, thus allowing free thermal expansion. These two conditions were also used with water-saturated specimens to investigate freeze-thaw phenomena. Haramis determined that cyclic temperature, under load, caused a reduction in strength for both saturated and unsaturated conditions. Results of this can be seen in section 4.1.

A similar investigation was done on the $(90,0,(\pm 45)_2,0,90)_{2T}$ laminate of vinyl ester/E-glass. The same four point bend apparatus used in Haramis' study was used in this study. Although both are vinyl ester/E-glass composites, the resin systems were different. Haramis used a Derakane 411-350 resin, where this study used a Derakane 441-400 resin. The apparatus consists of an aluminum frame with four aluminum bars

with load bearings. Strain gages applied to the center of composite specimens recorded strains of 4230 μm (± 170 μm).

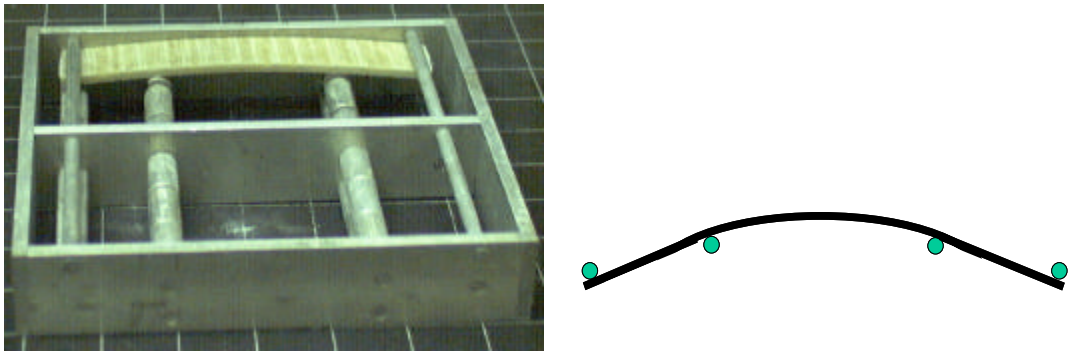

Figure 27. Four-point bend apparatus used in cyclic temperature tests.

Temperature was cycled between 0° and 100° F (-17.8° and 37.8° C) in order to mimic the maximum temperature range seen on the Tom's Creek Bridge. The temperature was cycled using a Blue M environmental chamber that uses a cascade refrigeration system and heating coils to change temperature. The temperature was ramped at a rate of 12.5° F per minute with a hold time of two minutes at 0° and 100° F. Each temperature cycle was completed in 24 minutes.

Loaded and unloaded specimens were placed in the Blue M environmental chamber for 100, 300, and 1000 temperature cycles. As a control, specimens were loaded for 5 and 24,000 minutes without temperature cycling. These last two conditions were to investigate initial damage caused by the four-point bend apparatus and any damage caused by time dependent mechanisms.

Chapter 4. Computer Simulation of Environ-mechanical Durability for Life Prediction on E-Glass/Vinyl Ester Composites using a Bridge Service Environment

4.1. Model Components

There has been a great deal of work on the individual components of environmental effects on composite material. Springer et al. studied temperature and moisture effects on composite materials. Heneff-Gardin et al. [29, [30] studied the effects of cyclic temperature on the distribution of stresses within a composite. Yet, few have looked at the combination of temperature, moisture, and load. Since the effects of the individual components have been well documented, another step is to combine these into a life prediction model. This section of study focuses on predicting the life of vinyl ester/glass composites during bridge service life conditions. The load and environmental history of the Tom's Creek Bridge of Blacksburg, VA will be used as a model. Data collected from sensors located on the Tom's Creek Bridge will be used to create a simulated year. Results from experiments, detailed in Chapter 3, will be used as elements in a computer simulation. These results will define:

1. Strength as a function of moisture content and temperature
2. Modulus as a function of temperature
3. Damage as a function of temperature and fatigue cycles

Life prediction and remaining strength models will be based on the critical element model. The information from the Tom's Creek Bridge will also be accelerated in an environmental chamber. By running fatigue tests at 14.75 Hz, the load cycles of one year are accelerated to just over six and a half hours.

4.1.1. Major Assumptions

Most engineering models and simulations begin their story with a number of assumptions or simplifications. The most significant simplification lies in the material difference between the Tom's Creek Bridge and the material used in this analysis. The Tom's Creek Bridge utilizes a hybrid composite of carbon and glass fibers with a vinyl ester matrix (Derakane 411-350). The shape is a double-web design with sub-flanges (Figure 28). The beam is predominantly glass fiber with carbon fiber tows dispersed in the flanges to provide greater flexural rigidity. Glass roving, 0/90° and ± 45° fabric, and continuous strand mat are utilized throughout the section. For the simulations, a different material system will be used. Instead of using a hybrid material and mimicking the lay-up of the beam, a quasi-isotropic laminate of glass and vinyl ester matrix was chosen to in order to simplify the model and analysis. The lay-up of the quasi-isotropic system is $(90,0,(\pm 45)_2,0,90)_{2T}$.

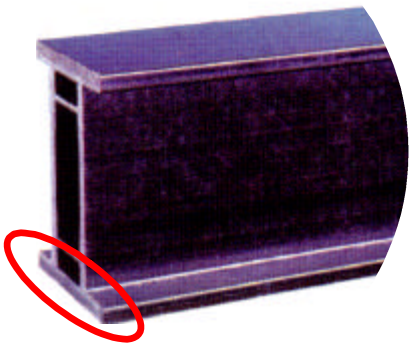

Figure 28. Beam used in the Tom's Creek Bridge. Tensile loads are greatest at the bottom flange.

This study will assume that the loading from each axle is a point load in the middle of the bridge. This is a conservative estimate, since cars normally do not drive on down the middle of the road. In reality, the loading of a vehicle will create normal and shear forces. To simplify the model, only the bottom flange of the beam will be analyzed

(Figure 28). From moment equations, this area exhibits the most tensile normal stresses. Also, the force will be assumed to create tensile stresses along the length of the beam. The stress is related to the load and place of loading from the following relationship:

$$s = \frac{My}{I} \tag{32}$$

The stress will be converted to a resultant force (Nx) for the model. A resultant moment is the force per unit length and can be calculated by multiplying the stress and the thickness of the composite. Combining all information, the resultant force is calculated by equation 33.

$$Nx = \frac{Myt}{I} \tag{33}$$

From bridge data; y is equal to 4 inches, the thickness (t) of the composite studied is .186 inches, and the moment of inertia (I) is 129.0 in^4. The moment (M) is equal to half of the load (P/2) multiplied by the distance to the center of the beam (120.625 inches). Substituting all of this into the resultant moment equals:

$$Nx = \frac{\left(\frac{P}{2}120.625\right)(4 \bullet .139)}{(129.0)} \tag{34}$$

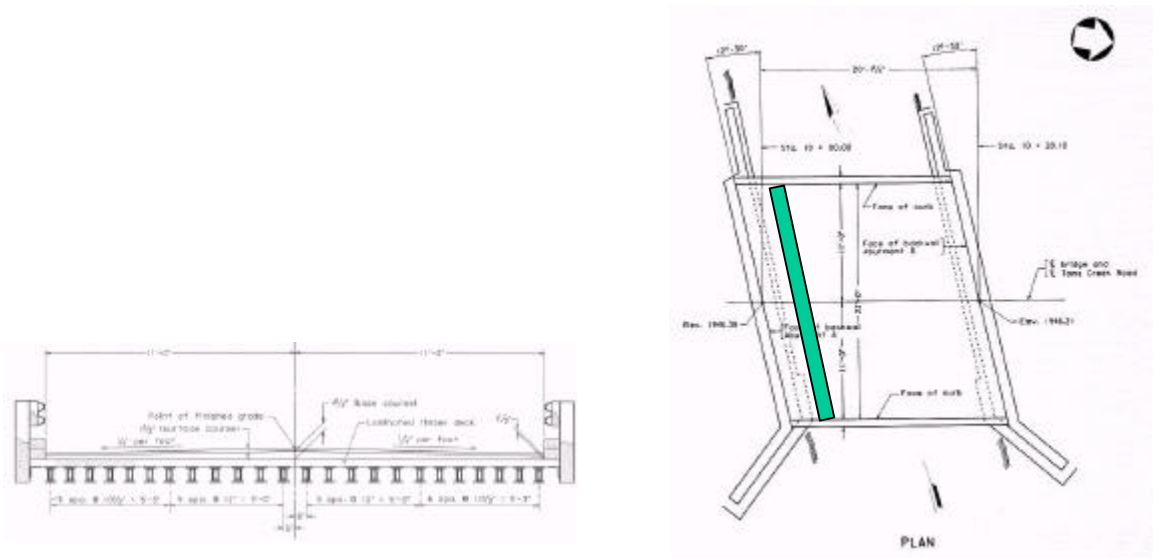

(a) (b)

Figure 29. (a) Side View and (b) Top view of Tom's Creek Bridge showing the location of the 24 composite stringers.

4.1.2. Vehicle Loading

The loading of a bridge is highly random and controlled by resident traffic. Although cars and trucks are the most frequent loads, light motorcycles to heavy five-axle trucks pass over the bridge. Thus, the model of the bridge must have variable loading as well. A load study measured the number and type of vehicles over the bridge during the different hours of a day.

Vehicle classes recorded were from motorcycles to five-axle semi trucks. From this data it was decided that two vehicle classes, Cars and Trucks/SUVs, would be used in the simulations. This decision was based on the size and frequency of loading. Motorcycles were not chosen as a load since few motorcycles cross the bridge each day, and their weight was relatively small. Vehicles with a weight over 15,000 lbs were not chosen since a stress conversion to the quasi-isotropic laminate would cause rapid failure.

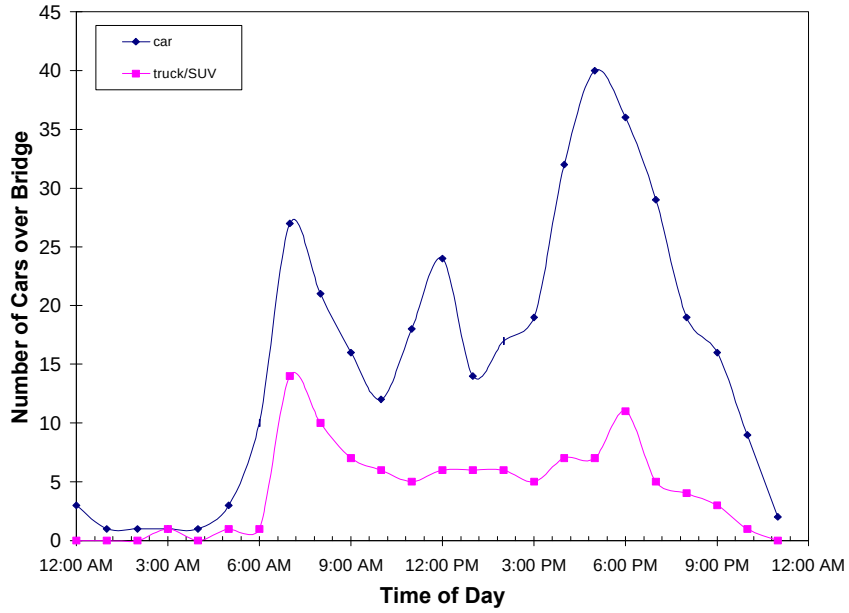

Figure 30. Number and cars and trucks/SUVs traveled over the Tom's Creek Bridge during a typical day.

The weights for cars, trucks and SUVs were determined by researching specifications of Ford and General Motors product lines. From this information, a weight of 3000 pounds will be used to represent a car and 5000 pounds to represent a truck or SUV. Since the number of motorcycles and large vehicles (Class 4 or greater) were relatively small, it was decided that for this study, only two different size loads would be used in the computer and laboratory simulation. These two loads would be based off of the number of cars and trucks/SUVs that passed over the bridge. Figure 30 depicts the number of cars and trucks/SUVs that pass over the Tom's Creek Bridge on an average day. The total number of cars and trucks that pass over the bridge on an average day is 106 and 371 respectively. Each time a vehicle drives over the bridge, each axle produces a load cycle. This study will assume that the weight is evenly distributed among the axles, thus a car, or truck, will have half of its load over each axle (Figure 31).

Figure 31. Vehicle loading for car (or truck/SUV). The load of the vehicle is assumed to be evenly divided among the axles.

The composite laminate theory, described in the literature review in chapter 2, was used to determine stresses through the $(0/90/(^{+}_{-}45)_2/0/90)_{2T}$ laminate of vinyl ester/ glass composite. For a "car load" of 1500 lbs, the σ_1 stress in the 0° plies is 170.45 ksi (see Figure 32). The stress distribution for a simulated "truck load" has the same shape as shown for the car load, except the values are greater. The σ_1 stress in the 0° plies for a truck load is 31.12 ksi.

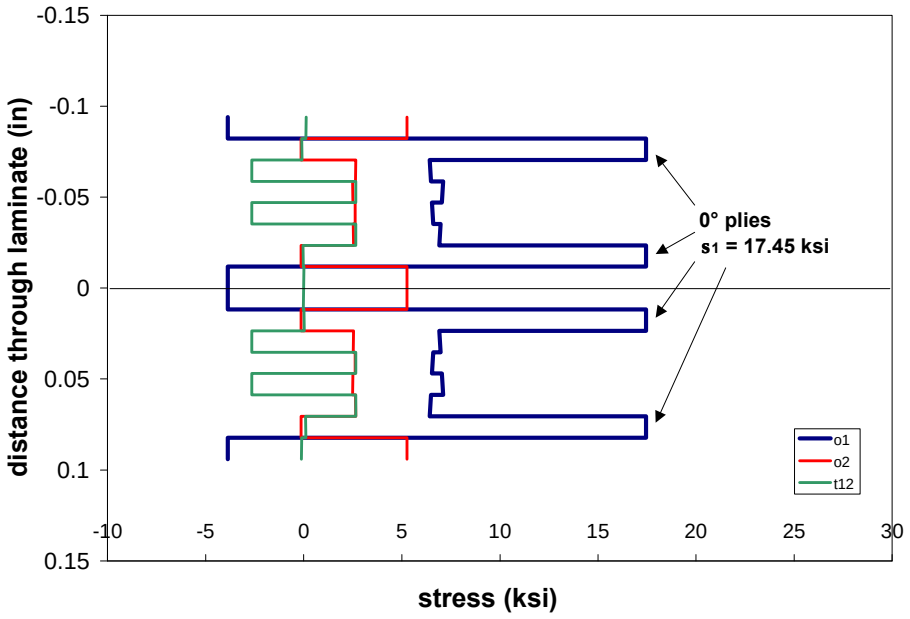

Figure 32. Stress distribution through $(0/90/(^{+}_{-}45)_2/0/90)_{2T}$ laminate due to a simulated "car load" of 1500 pounds. The σ_1 stress in the 0° plies is 170.45 ksi.

4.1.3. Life Prediction of Multi-Stress Block Loading

The fatigue life of vinyl ester/E-glass composite was investigated. Using previous remaining strength data, the number of cycles at which 60% of the ultimate tensile strength remained was determined for loads of 28.8% and 40.6% UTS. At the higher load of 40.6% UTS, it was determined that 6734 fatigue cycles would decrease the strength to 60% UTS, where as the lower load required 518,100 cycles. This information was then used to draft two different tests. In one, specimens were fatigued at the high load for 6734 cycles, then fatigued until failure at the lower load. Using a remaining strength analysis, the strength of the composite should follow the path seen in Figure 33. The lower load is predicted to fail in 488,634 cycles.

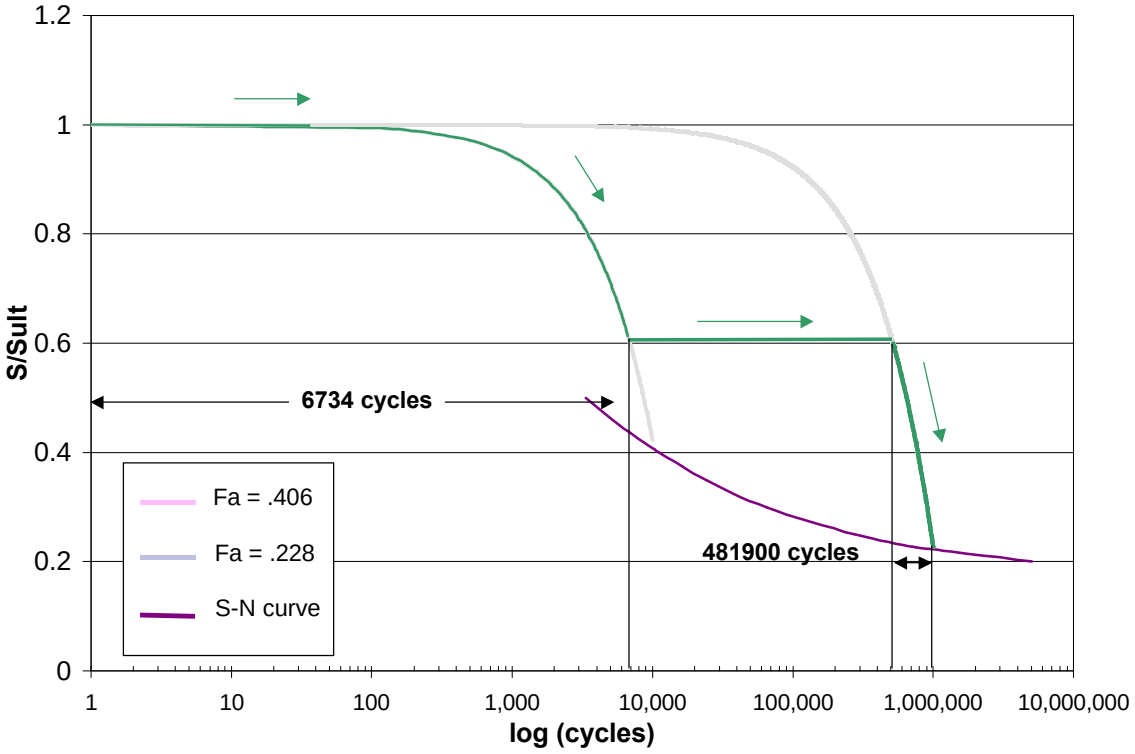

Figure 33. Remaining strength path for quasi-isotropic laminate fatigued at 40.6% UTS for 6734 cycles followed by fatigue at 22.8% UTS until failure. Remaining strength curves for 40.6 and 22.8% UTS are shown as pink and blue lines respectively. The S-N curve is shown in purple.

Another investigation began by fatigue cycling at the lower 22.8% UTS until 60% of ultimate tensile strength remained (after 518,100 cycles). The load was then increased to 40.6% UTS where it is predicted to fail after 3072 cycles. The remaining strength path, shown in Figure 34, can be determined using the remaining strength model. Failure life using the remaining strength model for this load scenario is predicted at 521,172 cycles. The high-low condition has a longer life prediction.

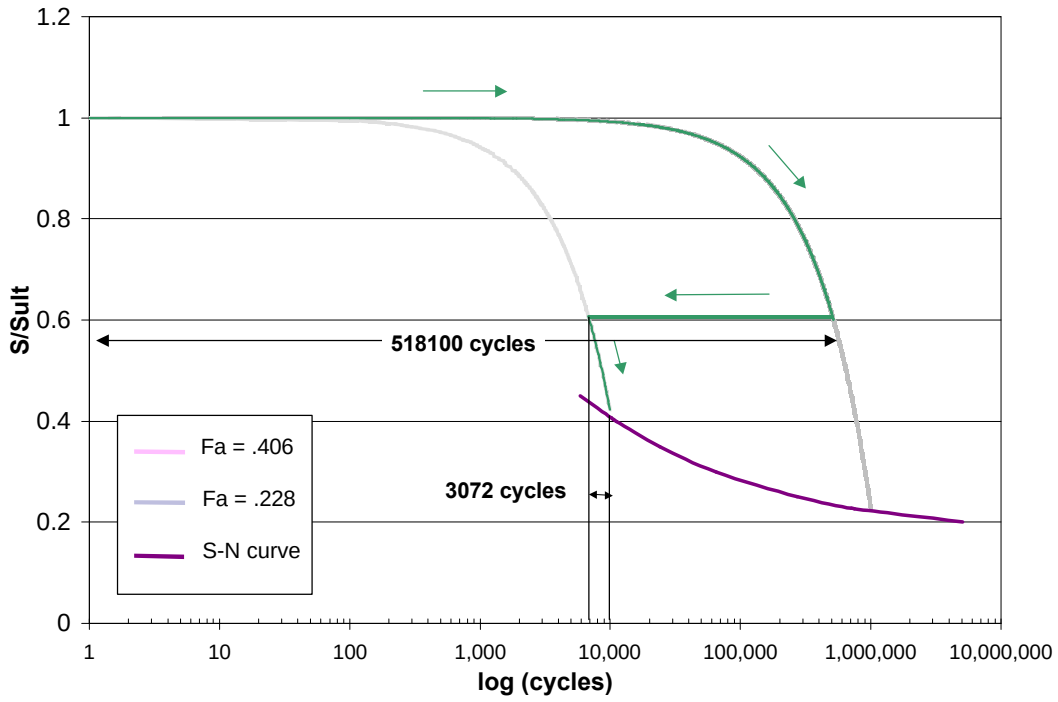

Figure 34. Remaining strength path for quasi-isotropic laminate fatigued at 22.8% UTS for 518,100 cycles followed by fatigue at 40.6 % UTS until failure. Remaining strength curves for 40.6 and 22.8% UTS are shown as pink and blue lines respectively.

Fatigue tests were done on a MTS servo-hydraulic test frame under load control. The R ratio, or minimum load divided by maximum load, was kept at 0.1. Specimen preparation is described in section 4.1. Results were compared to the prediction scheme mentioned above and Miner's Rule. Miner's Rule for each multi-stress block load condition is calculated. The results for the experimental data, critical element model prediction and Miner's Rule are tabulated in Table 3.

Table 3. Results from experimental data, critical element model prediction and Miner's Rule for each multi-stress block load condition.

		cycles at	cycles at	Total
	Specimen	Fa = .228	Fa=.406	Cycles
High-Low	Average	504,088	6,734	504,088
	Predicted	481,900	6,734	481,900
	Miners	345,133	6,734	345,133
Low- High	Average	518,100	211	518,311
	Predicted	518,100	3,072	521,172
	Miners	518,100	4,819	522,919

The average values for both load scenarios were close to the predicted value. There was some scatter in the high-low condition, but the scatter was under a decade. For the low-high condition, the data, critical element model prediction and Palmgren-Miner's Rule prediction all overlapped. These results can be seen in Figure 35.

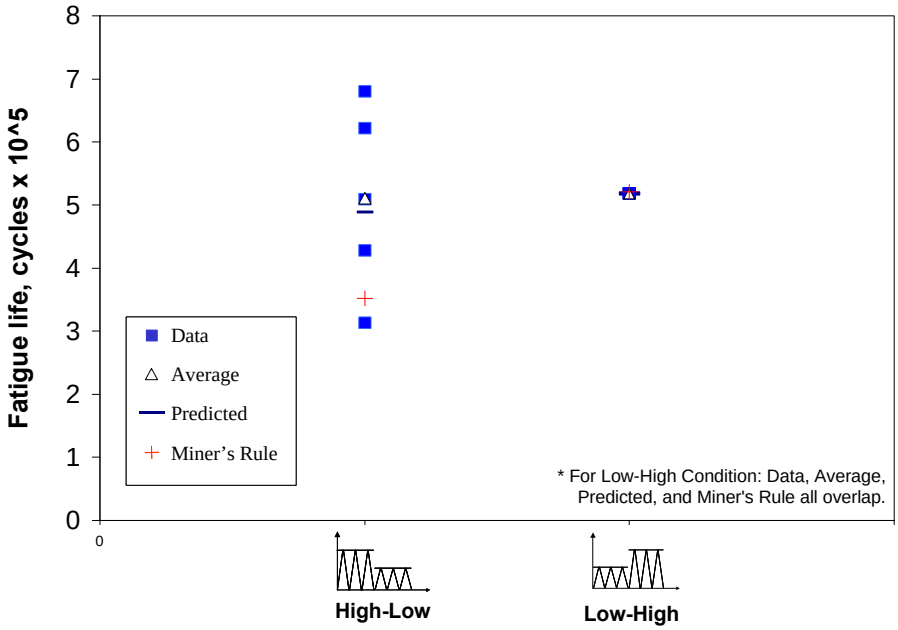

Figure 35. Results from block load investigation. The prediction using the critical element model is more accurate than the Miner's Rule. Note also that the data, predicted value, and Miner's Rule vale for the low-high condition overlap.

At first glance, the High-Low condition (Figure 35) appears to have a larger amount of scatter than the Low-High condition. In reality, the scatter of the Low-High condition is greater. This can be seen by comparing the second block load. The predicted value of the high load of the Low-High condition was 3,072 cycles, but the average failure time was only 211 cycles (Table 3). This is a difference of over one decade. The difference in predicted and failure for the High-Low condition was less than a tenth of a decade.

These differences in scatter may be a function of the failure mechanisms of the specimens. Images of the failed specimens of the High-Low specimens (Figure 36) show some failures with little fiber pullout. The thought is that the initial high cyclic loads cause damage in regions of weaker material (i.e. localized flaws). As the load is lowered, the damage continues to accumulate at this relatively small region until failure, and creates less fiber pullout than the Low-High condition. Images of the failed specimens of the Low-High condition (Figure 37) show a larger amount of fiber pullout. The failure mechanisms are different in that low cyclic loads disperse damage over a relatively large region. When the load is increased, the high cyclic loads then finally fails the specimen by bridging these damaged areas and causing fiber pullout. The conclusion is that the High-Low condition will show larger amounts of scatter since the initial failures are a function of localized flaws, whereas the Low-High condition disperses the damage over a larger area and damage is on a more global scale.

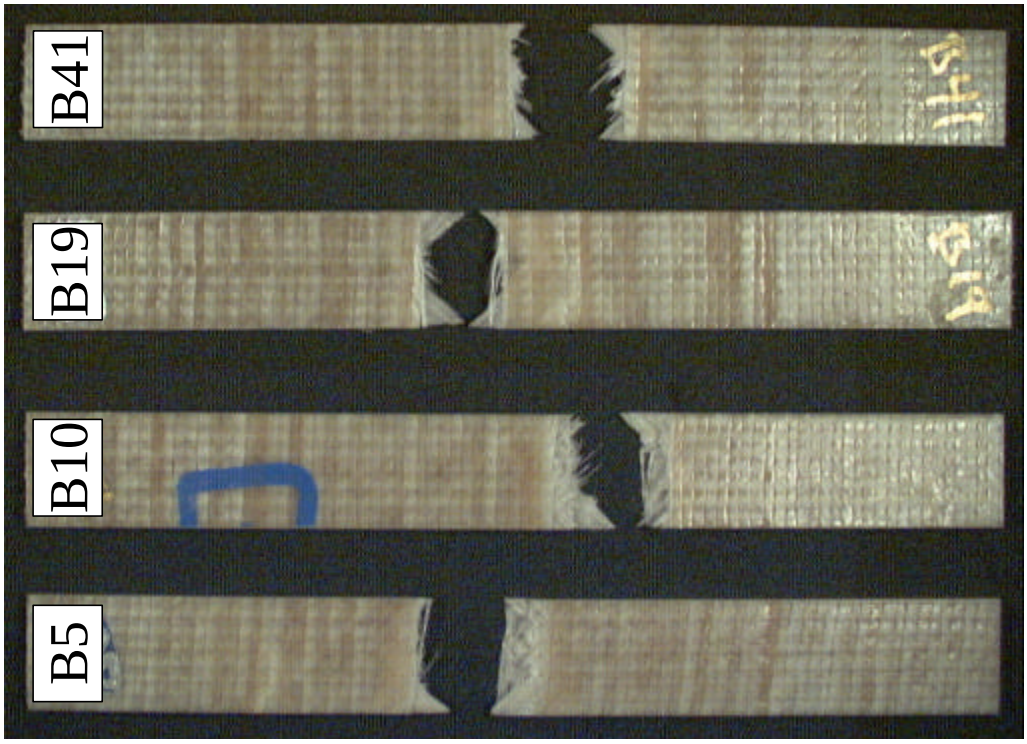

Figure 36. Failed specimens for the High-Low condition. Note that the specimens show little fiber pullout.

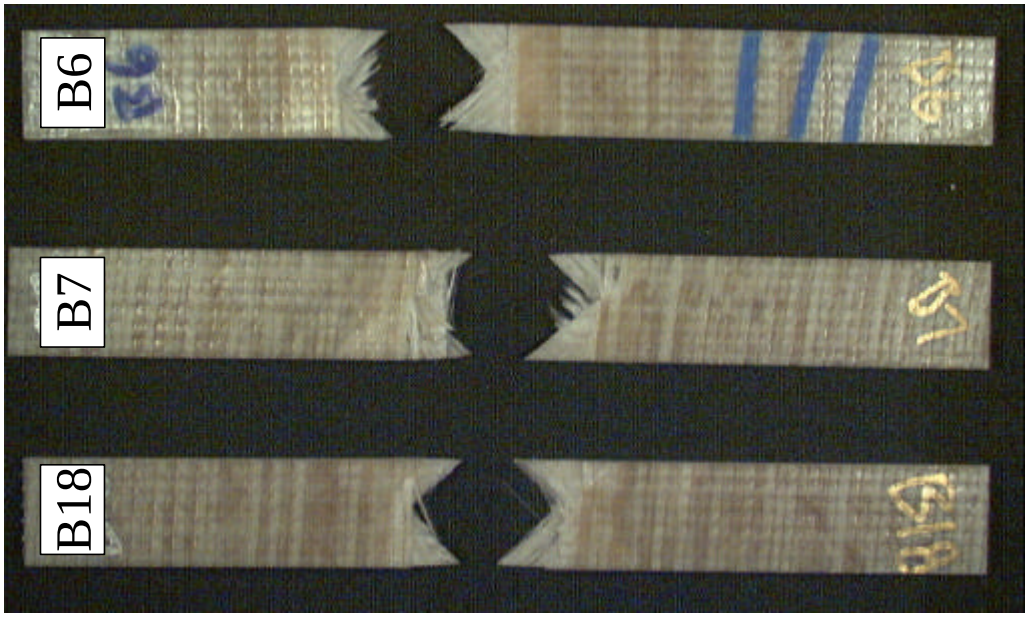

Figure 37. Failed specimens for the Low-High condition. Note that there are significant amounts of fiber pullout.

Another possible reason for the disparities between predicted and experimental results may be linked to the condition at the change in load. Testing equipment often produces inaccurate load cycles directly after a sudden change in load. For low-high cases, an overshoot in load can cause a large decrease in remaining strength, thus producing failures sooner than predicted. For Low-High cases, a little different explanation is possible. At low loads, such as 22.8% UTS in this study, the slope of the S-N curve is more shallow. Thus, a slight change in load level results in a large change in failure life. Thus, any load variations may produce large differences between predicted and experimental results.

In both load scenarios, the critical element model closely predicted the results from the experimental data. Both the Miner's Rule and critical element model gave conservative predictions for the high-low condition and non-conservative predictions for the low-high scenario. Miner's Rule was the least accurate for both scenarios, predicting failure as much as 159,000 cycles earlier than the average experimental data for the high-low condition showed. Literature has shown that Miner's Rule is often conservative in high-low block load scenarios and non-conservative for low-high conditions [41].

The results from this section show that the vinyl ester/glass composite system used in this study gave very accurate correlations between predicted and experimental results for the high-low condition. One of the objectives of this study was to determine if life could be predicted from multi-stress load patterns by looking at fundamental block loading cases. The load pattern for the laboratory simulation in the following section is a little more complicated as it uses a repeated block of seven low loads and two high loads. Since the critical element model used here was able to predict the lifetime for two level multi-stress block loading, it is hypothesized that the critical element model will predict lifetime using a small repeated block loading situation.

4.2. Temperature

4.2.1. Data From Tom's Creek Bridge

The Tom's Creek Bridge is located in Blacksburg, VA. Blacksburg has four distinct seasons. Temperature sensors have been placed on the bridge and have been monitoring bridge temperature. Results of the temperature sensors are seen in Figure 38. The summers are hot and humid with average temperatures ranging from 60 to 80 °F. Winter season includes average temperatures from 32 to 38 °F, but has many days that fall below freezing. Fall and spring seasons are transitions between winter and summer.

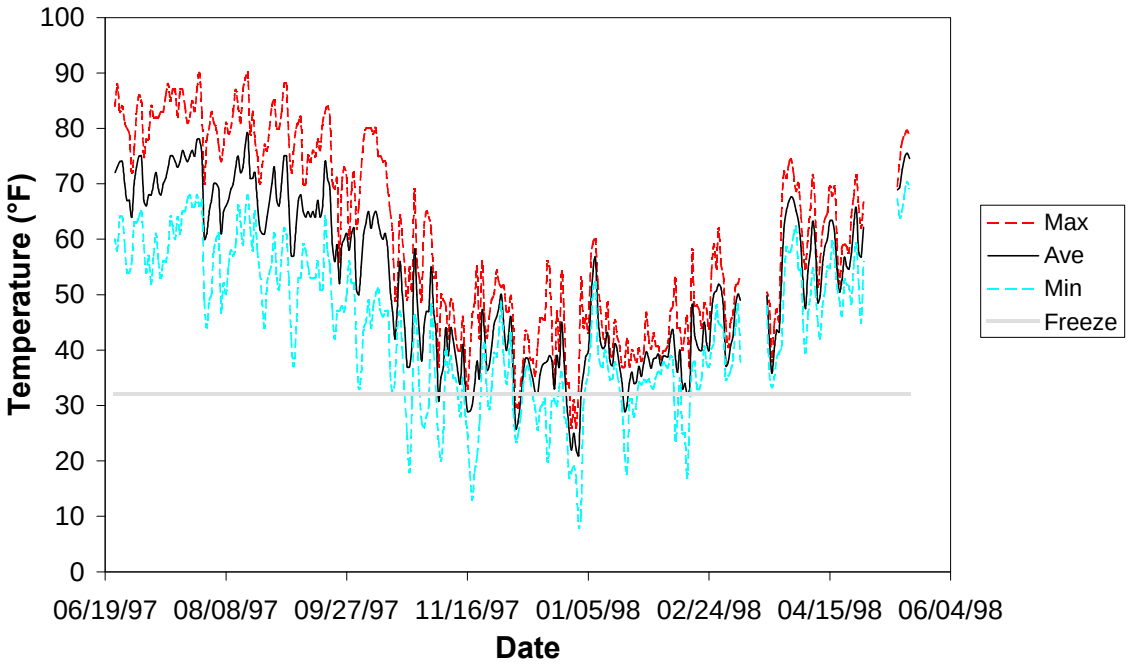

Figure 38. Maximum, minimum, and average temperature of each day seen on the Tom's Creek bridge over one year.

4.2.2. Humidity and Temperature Simulation

Original ideas for modeling the temperature included a sine wave pattern for representing the change in temperature over a given day. Since it was determined experimentally that cyclic temperature over the range of 100° F showed no reduction due to cyclic damage, it was decided to keep temperature constant over a simulated day. Even though there is a change in strength with temperature over the range of 20° F, one of the goals is to accelerate testing to predict fifty-year lifetime. Holding at a constant temperature would allow for quicker experimental testing. Extreme temperatures were used in order to yield conservative results. The data shown in Figure 38 shows a high of 92° F and a low of 8° F. For the simulations, a range of 0° to 100° F was used. Winter and summer months would consist of a constant temperature at 0° and 100° F respectively. For fall and spring seasons, a steady ramp connected the winter and summer months. A schematic of this situation is shown in Figure 39.

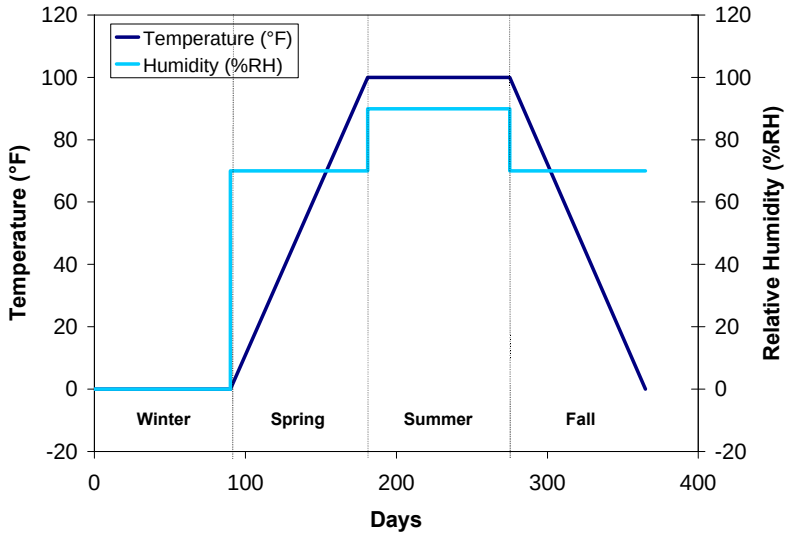

Figure 39. Schematic of temperature and humidity model used in laboratory and computer simulation.

4.2.3. Strength as a Function of Temperature

The strength of the composite was found to decrease with increasing temperature. The results can be seen in Figure 40. The tensile strength data was normalized to room temperature. A linear fit gives a slope of 0.135% change per degree Fahrenheit, thus over the 100° range, a 13.5% change in strength is seen. This relationship will be used later in the computer simulation.

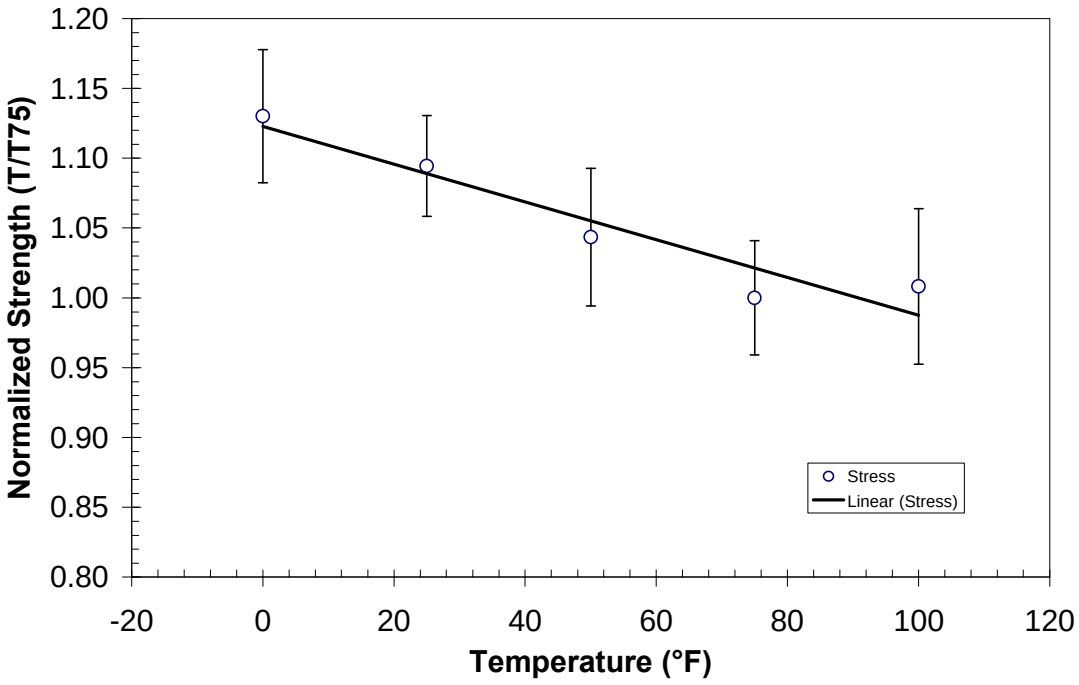

Figure 40. Normalized tensile strength as a function of temperature. The curve is normalized to room temperature (75° F).

4.2.4. Cyclic Temperature Testing

Cyclic temperature tests show no change in strength properties with number of temperature cycles (Figure 41). Cyclic temperature was done between 0° and 100° F under a four point bending load. Strain gages attached to the composite determined a bending strain of 4230 μm ($^{+}$- 170 μm). As seen in Figure 41, a linear trend line does

show a slight increase in strength with cyclic temperature. This increase in strength, due to the cyclic temperature, is not statistically accurate due to the error bars.

As a control, specimens were loaded in the four point bend apparatus, without cyclic temperature, for 5 minutes and 2400 minutes. Both tests were performed at room temperature. The five-minute test was performed to determine if the four-point bend loading caused any irreversible damage. No noticeable strength change was seen. The 2400-minute test was performed to see if damage occurred over the time duration of 1000 temperature cycles. Again, no noticeable strength change was seen.

The cyclic temperature experiment was also performed without load. Specimens were placed in a rack that allowed for free thermal expansion. Again a trend line indicated a slight increase in strength, but the change was not outside statistical boundaries.

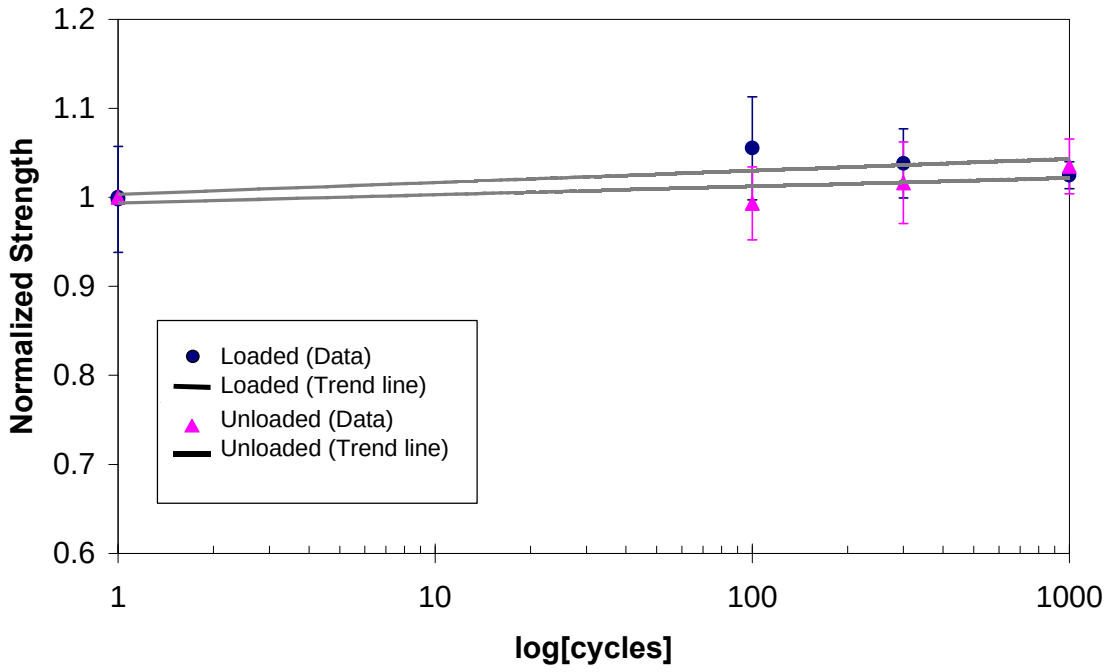

Figure 41. Normalized strength as a function of cyclic temperature (0° to 100° F) under loaded and unloaded conditions.

Originally, it was assumed that temperature cycling would cause damage in a vinyl ester/E-glass composite. Haramis showed microbuckling with a Derakane 411-350/E-glass composite under similar conditions [23]. This was not the case in the Derakane 441-400/E-glass composite of this study. The difference in response may be found by comparing the resin properties.

4.2.5. Modeling for Temperature

Strength was found to be a function of temperature. Between the 0° and 100° F temperature range is a 13.5% difference in strength. This will change the lifetime of the composite material. The strength values were normalized to room temperature strength. A linear plot of the normalized data shows a linear trend line (see Figure 4) with an equation of the form:

$$S_n = -0.0013539\ T + 1.1229453 \qquad (35)$$

Where S_n equals the normalized strength (normalized to room temperature) and T equals temperature in degrees Farenheit. Actual strength values at a given temperature are found by multiplying the S_n value by the room temperature strength of 37.32 ksi.

The modulus of the neat resin was shown in an independent study by Phifer et al. [28] to change as a function of temperature. The data was normalized to room temperature data. A bi-linear curve was used to model the change in neat resin modulus as a function of temperature (Figure 42). Actual modulus can be determined by multiplying the normalized value by the room temperature value of This modulus is then used to determine the transverse modulus in the off-axis plies by using Halpin-Tsai micromechanics and assuming that the fiber stiffness does not change.

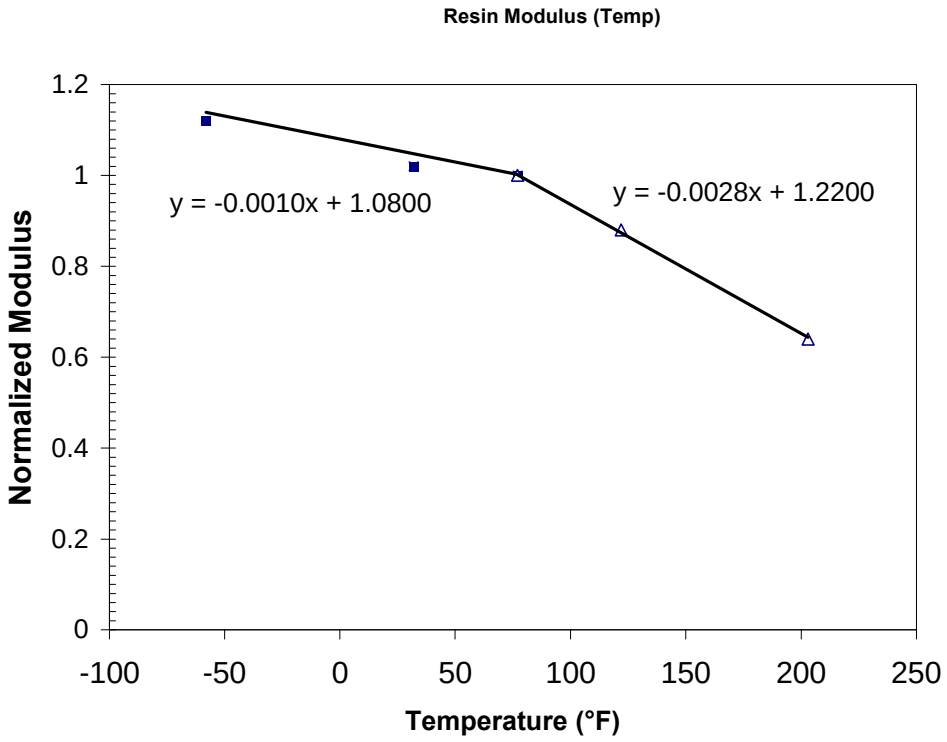

Figure 42 Neat resin modulus as a function of temperature (°F). Data was determined in an independent study by Phifer et al [28].

4.3. Moisture

4.3.1. Moisture Uptake Study

Specimens were aged in water at 95°, 113°, 131°, and 149° F (35°, 45°, 55°, and 65° C) in water. Relative moisture uptake measurements were taken at regular intervals. Since it is common to display moisture uptake plots on a square root[time] scale, moisture measurements were made frequently during the beginning of the analysis and less often as time progressed. The results can be seen in Figure 43.

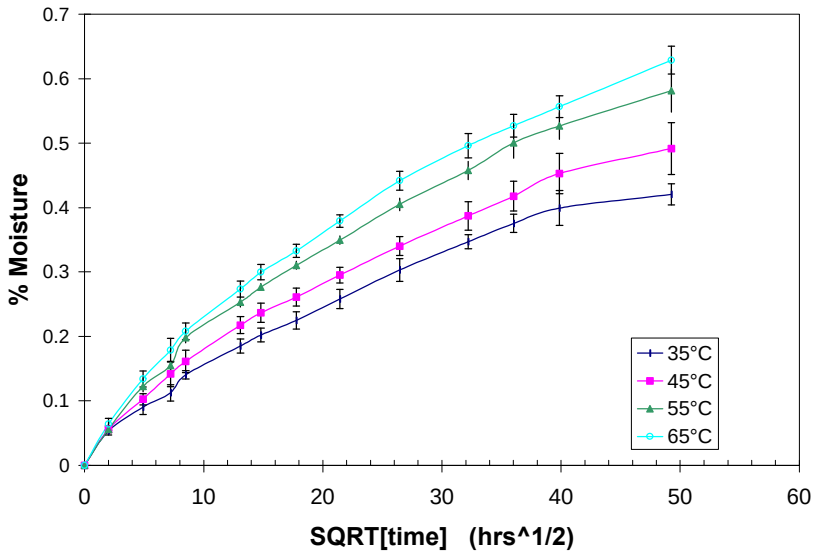

Figure 43 Moisture uptake for vinyl ester/E-glass composite at 95°, 113°, 131°, and 149° F in water.

The results show that higher temperatures have a steeper slope and higher maximum moisture content. Fick's law compares well with initial moisture uptake. The initial slopes of these curves were used to determine the activation energy and diffusion coefficient. Using equation 31 to determine the diffusion constant (D) for each temperature and plotting ln D vs. 1/T gives Figure 44. The activation energy and diffusion coefficient are calculated as 3527 cal/g-mol and 0.033 cm^2/sec. These values will be used later in the computer simulation.

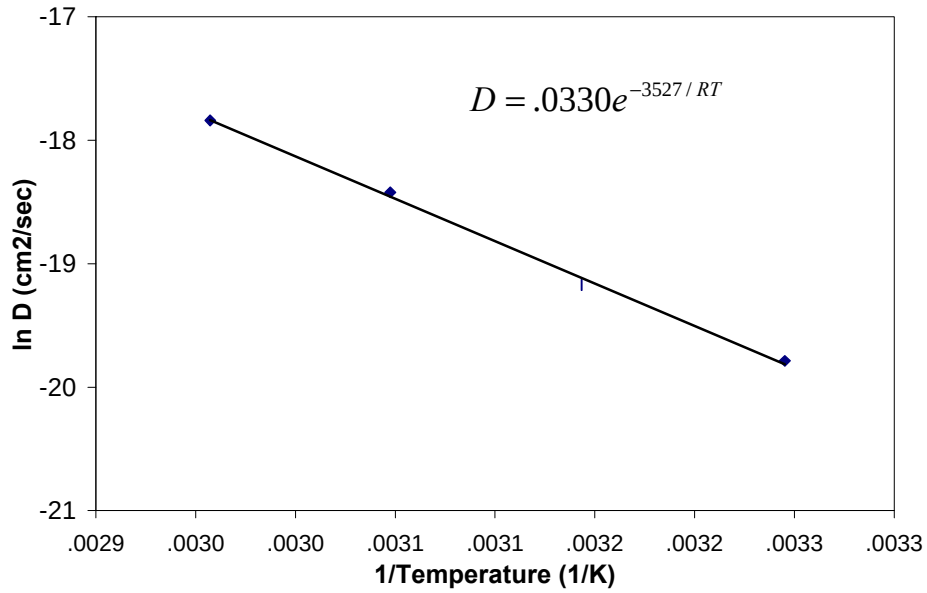

Figure 44. ln(D) vs. 1/T for determination of activation energy (E_d) and diffusion coefficient for $(90,0,(\pm 45)_2,0,90)_{2T}$ laminate of vinyl ester/E-glass pultruded composite.

4.3.2. Residual Tensile Properties after Moisture Exposure

Tensile strength was determined as a function of moisture content (Figure 45). Aging was done at 149° F (65° C) until moisture content reached 0.15, 0.30, 0.45, and 0.60% relative moisture. The results show that initially, strength increases with moisture content. This may be due to increased cure of resin from temperature of water bath or moisture swelling may reduce stresses caused form cure shrinkage. After 0.15% relative moisture content, the strength of the composite drops to 69% of as-received tensile strength at 0.60 % relative moisture.

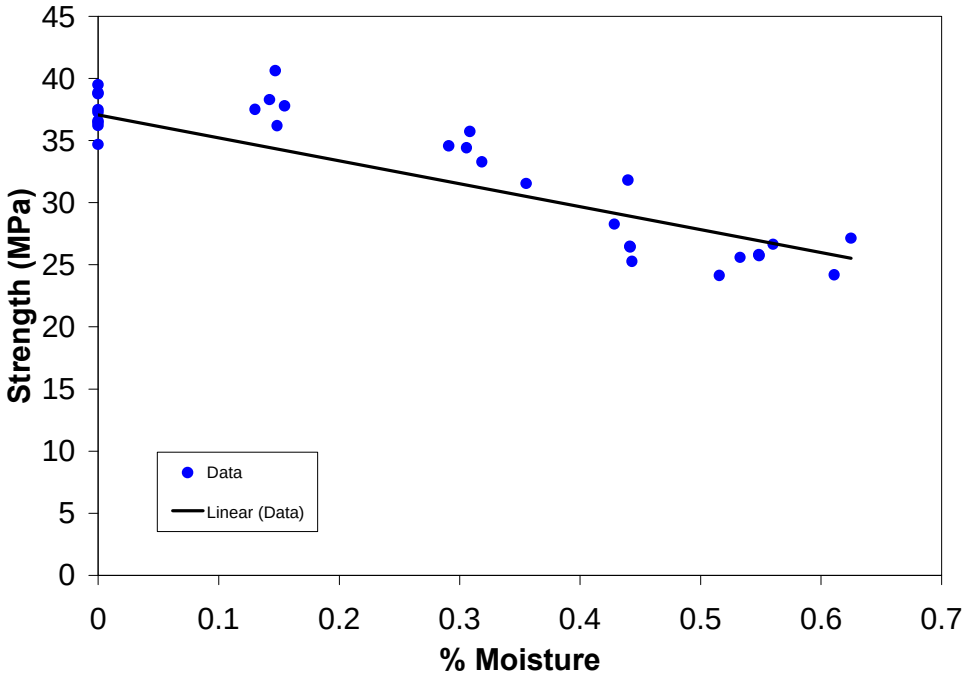

Figure 45. Strength as a function of moisture content using a linear trend line.

The effect of aging temperature was studied by aging the composites to 0.30% relative moisture at 95°, 113°, 131°, and 149° F. Thus, the composites were soaked at various aging times. The results showed no significant change in tensile strength as a function of iso-moisture conditions (Figure 46). Therefore, the strength of this composite is a function of moisture content, not aging time or temperature.

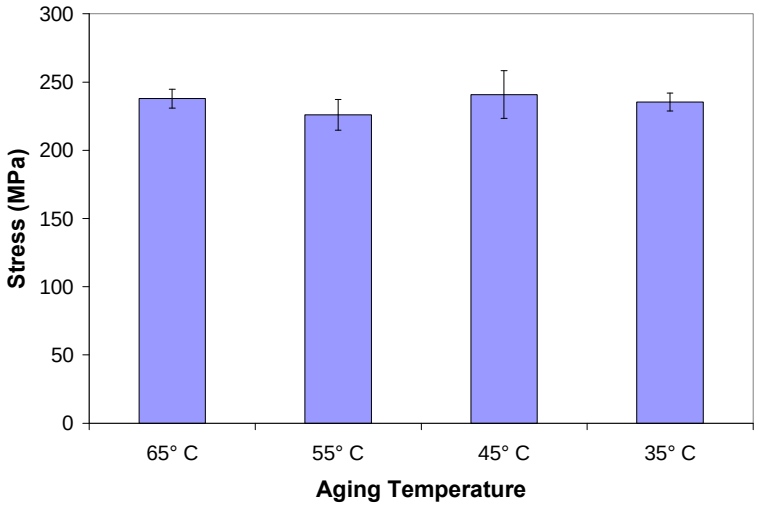

Figure 46. Tensile strength as a function of aging temperature. The composite specimens were aged at 35, 45, 55, and 65° C until moisture reached 0.30 % relative moisture.

4.3.3. Fatigue Properties: Aged S-N Curve

The effect of moisture on fatigue properties was determined by creating an S-N curve. Composites were aged at 149° F until 0.60% moisture content was reached. The results of the fatigue testing can be seen in Figure 47. The curve shows an increase in life with decreasing stress level at a slope of 10.6% per decade. This slope falls within Mandell's stipulation for fatigue life of glass fiber composites of 10-11% per decade [25] [26]. Runout specimens, two million cycles without failure, were found at 35% UTS.

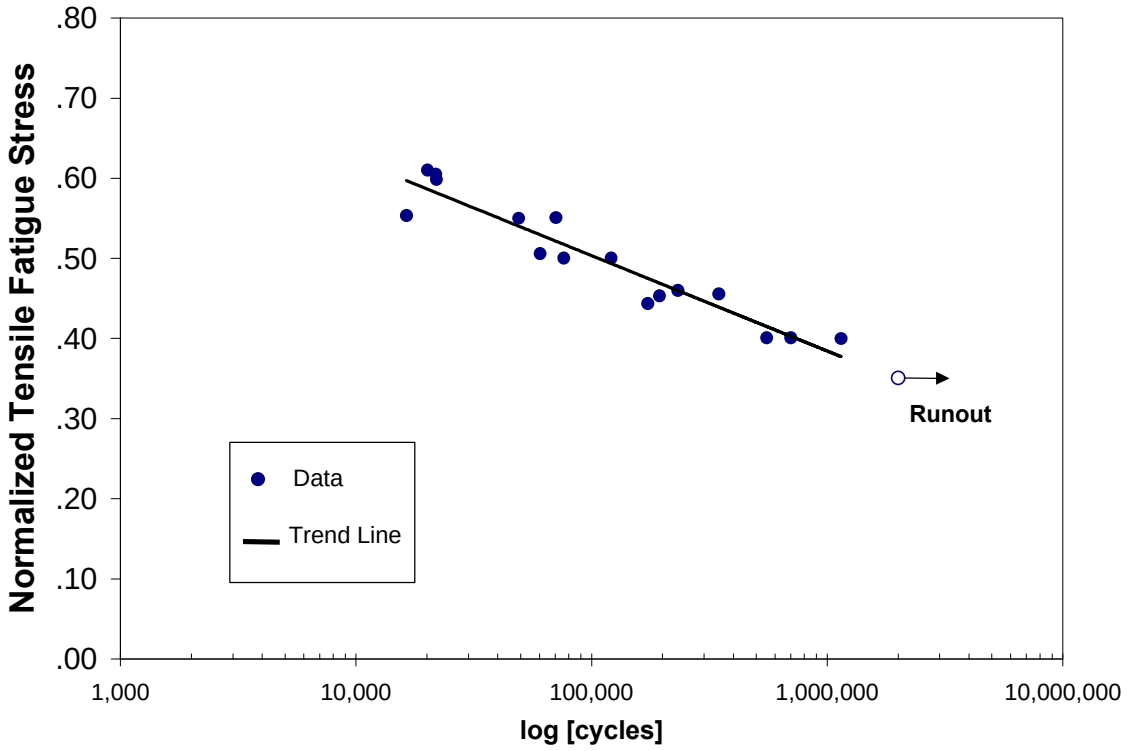

Figure 47. Normalized tensile fatigue stress vs. number of cycles to failure for quasi-isotropic laminate aged until 0.60% moisture content.

4.4. Modeling for Moisture: Finite Difference Method

As stated earlier, the presence of moisture changes the mechanical properties of a material. These changes are relative to the amount of moisture in the material. Prior to saturation, there is a moisture gradient through the material, thus there is a property change through the material. Earlier, Fick's law of diffusion was discussed with explanations on how to solve for moisture content as a function of time. This method is only applicable for situations of constant boundary conditions of temperature and humidity. This is not the case for the service conditions of the bridge where temperature and humidity are changing constantly. Therefore we need to be able to calculate moisture profiles with changing humidity and temperature.

To begin this, one must first understand what is happening as a function of the changing boundary conditions. We know from earlier sections that diffusion constant is a function of temperature and can be expressed using the Arrhenius type equation:

$$D = D_o \exp(-E_d / RT) \tag{36}$$

where E_d, D_o, R, and T are the activation energy, diffusion constant coefficient, universal gas constant, and temperature in degrees Kelvin respectively. From experiments, we determined the diffusion coefficient and activation energy earlier. Now that the diffusion constant can be written as a function of temperature, and maximum moisture boundary conditions are defined by humidity, one can now solve for changing boundary conditions. An excellent method for use with computational models is the finite difference method. The material element is first discretized into small elements. The boundary conditions are then applied at the left and right side of the material. The equation for the right side is given by:

$$Q_j^{n+1} = \frac{\frac{Q_j^n}{\Delta t} + \frac{2D_j Q_{j+1}^{n+1}}{\Delta x_j\left(\Delta x_j + \Delta x_{j+1}\right)} - \frac{2D_{j-1}\left(Q_j^n - Q_{j-1}^n\right)}{\Delta x_{j-1}\left(\Delta x_j + \Delta x_{j-1}\right)}}{\left(\frac{1}{\Delta t} + \frac{2D_j}{\Delta x_{j-1}\left(\Delta x_j + \Delta x_{j-1}\right)}\right)} \tag{37}$$

and from the left side by:

$$P_j^{n+1} = \frac{\frac{P_j^n}{\Delta t} + \frac{2D_j\left(P_{j+1}^n - P_j^n\right)}{\Delta x_j\left(\Delta x_j + \Delta x_{j+1}\right)} + \frac{2D_{j-1}P_{j-1}^n}{\Delta x_{j-1}\left(\Delta x_j + \Delta x_{j-1}\right)}}{\left(\frac{1}{\Delta t} + \frac{2D_{j-1}}{\Delta x_{j-1}\left(\Delta x_j + \Delta x_{j-1}\right)}\right)} \tag{38}$$

where Q and P are the concentration. There will be a small amount of error from the two solutions. Therefore, the final solution is given by averaging the two. The solution can be seen schematically in Figure 48 as a function of position at different times.

$$C_j^{n+1} = \frac{P_j^{n+1} + Q_j^{n+1}}{2} \tag{39}$$

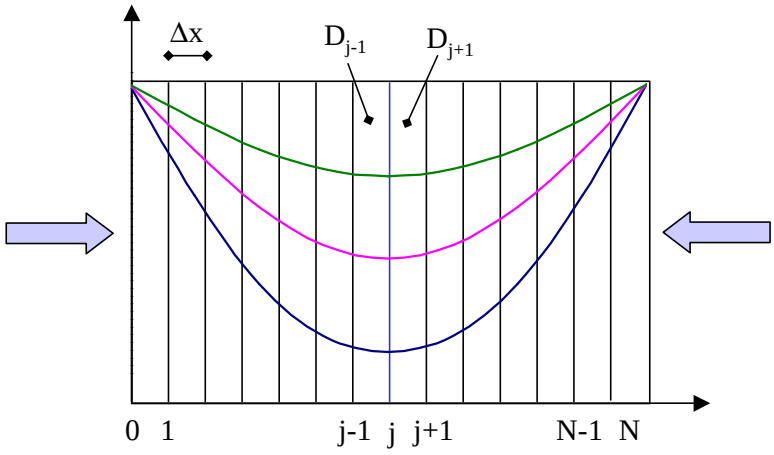

Figure 48. Schematic showing discretization of material in which moisture absorbs from the left and right sides.

This method of solving the differential diffusion equation has many strengths. Not only can it solve for changing moisture and temperature, but it can solve for composites with ply-by-ply diffusion constants. Other researchers have investigated moisture absorption using this method with great success. George Springer et al. has created a software program (W8GAIN) that solves the differential equation using the finite difference method [6]. Aditya and Sinha investigated the diffusion coefficients during cyclic exposure [49]. Their focus was aimed at determining diffusion coefficients for the steady state situation from data generated during cyclic exposure. Even during cyclic environment, a linear, nonlinear, and saturation regions were seen. Adda-Bedia et al. investigated the fluctuating moisture concentration found at the upper surface of the material [50]. Due to changing maximum moisture boundary conditions, there will be a time when there is a more moisture inside the composite. During this time the composite desorbs. Adda-Bedia et al. showed that outer layers of the composite show a fluctuating moisture concentration due to the changing boundary conditions, while inner layers were more stable.

This type of solution requires boundary moisture content in terms of maximum possible moisture that can be achieved by the composite. Verghese et al. [35] showed that moisture concentration from relative humidity can be converted to a maximum moisture content. For vinyl ester glass systems, it follows a power law form in which a and b are .653 and 4.3 respectively (equation 40). Experimental work has not been done to determine the constants for the $(0/90/(^{+}_{-}45)_2/0/90)_{2T}$ laminate of vinyl ester/ glass composite. For the computer simulation used here, the constants .653 and 4.3 will be used for a and b respectively.

$$M_{\max} = a(RH)^b \tag{40}$$

Strength of the vinyl/ester composite system was also determined as a function of moisture content using a linear trend line. Results from water bath aging at 65° C showed a decrease in strength as a function of increasing moisture (Figure 45). The results can be modeled using a linear trend line to equal an equation of the form:

$$S_T = -18.47(M) + 37.07 \tag{41}$$

Where S_T is the tensile strength (ksi) and M is the relative moisture in percent.

4.5. Damage Accumulation Model

Fatigue loading is known to cause matrix cracking in the off axis plies. Results from Phifer [24] determined the reduction in off-axis stiffness as a function of fatigue loads. It can be modeled using a linear trend line to give the equation:

$$\frac{E_2(n)}{E_2(q.s.)} = -.317\left(\frac{n}{N}\right) + .6427 \tag{42}$$

Where $E_2(n)$ and $E_2(q.s.)$ are the off axis modulus at a given fatigue cycle and from quasi-static data respectively. The data for this is shown in Figure 49.

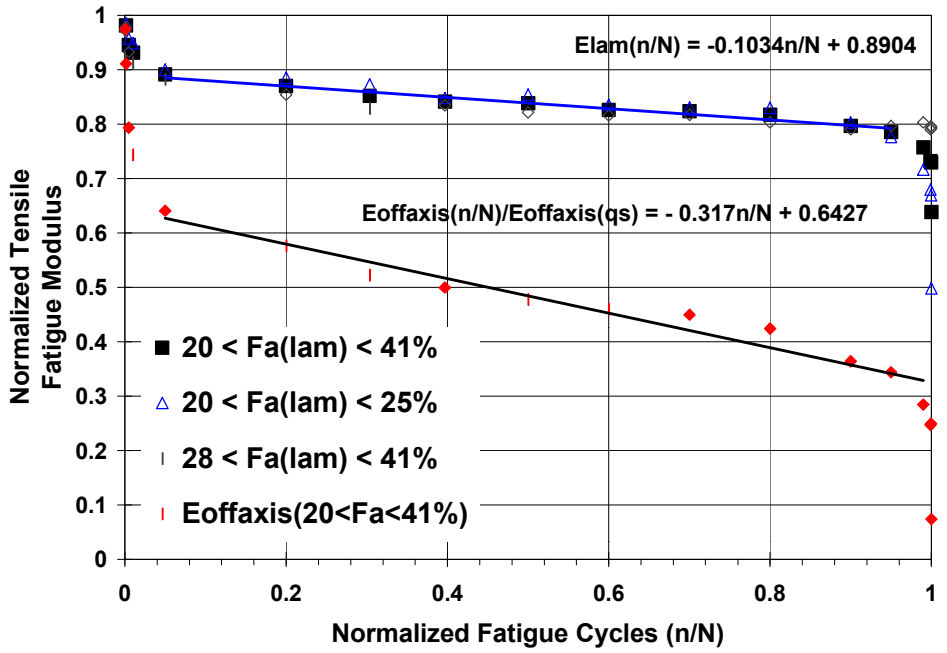

Figure 49. Normalized Tensile Fatigue Off-Axis Modulus Reduction for QI1. (Data courtesy of S. Phifer [3]).

4.5.1. Computer Simulation Summary and Flow Chart

The computer program consists of three steps; temperature, humidity, and vehicle loading. The computer program begins on the first day of winter and cycles through the seasons. For each day a temperature and humidity are defined followed by damage from vehicular loading. The temperature of a given day is determined, which is used to calculate the transverse modulus in the off axis plies using micromechanics. Strength is then determined as a function of temperature. Using the Arrhenius equation and diffusion coefficient and activation energy determined experimentally for the vinyl ester/glass composite, the diffusion constant is calculated for the given temperature.

A finite difference method is used to calculate a moisture gradient due to humidity. The strength and modulus of each ply is then reduced as a function of the moisture concentration. Vehicle type and number of loading is then defined. The loading creates damage accumulation in the form of matrix cracking and off axis stiffness

reduction. Composite laminate theory (CLT) is then used to determine the stress state of each ply. The stress in the 0° plies and the strength determined from the environmental state (Xt) are then used to determine the failure function, Fa. The remaining strength is then calculated using the critical element model. This completes one cycle within the program. New material properties are then set before looping back through the program. This scheme is shown in a flow chart in Figure 50.

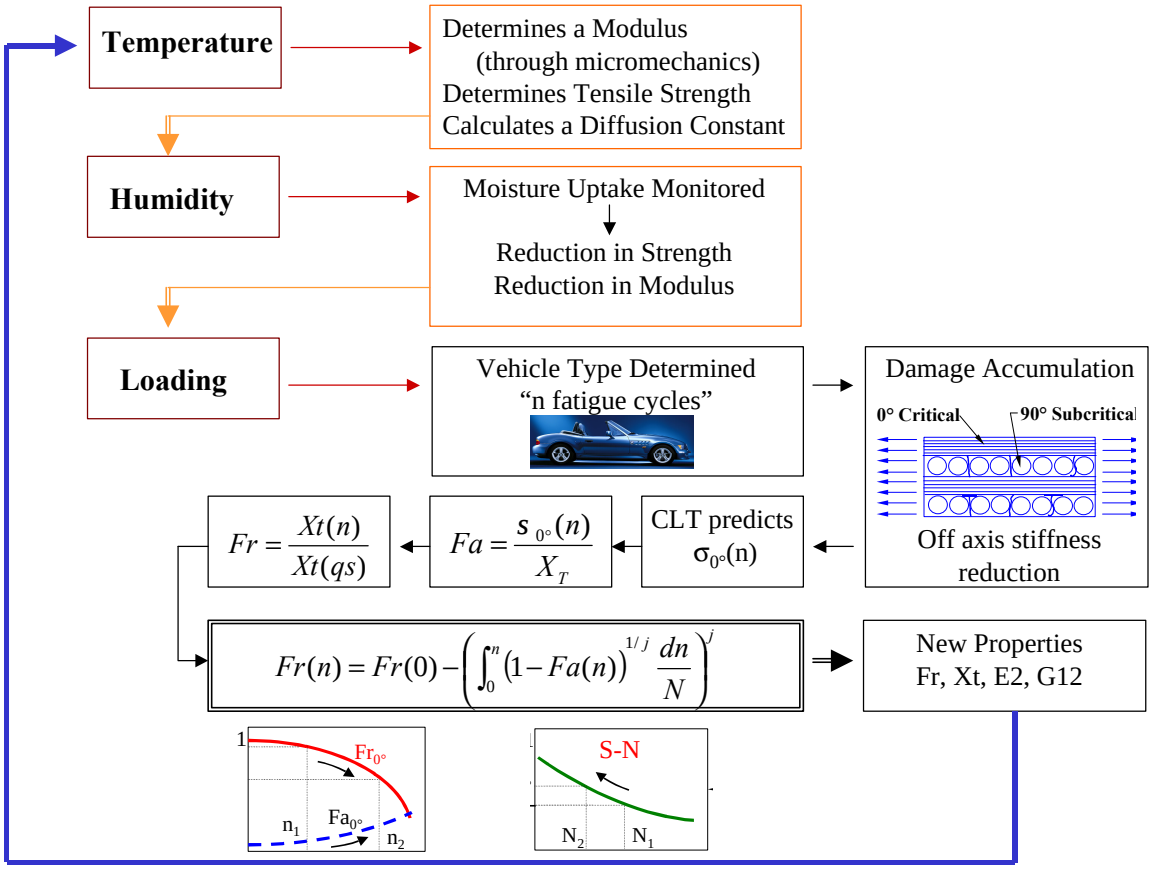

Figure 50 Flow chart showing the procedure used in the Computer Simulation

4.6. Results of Computer Simulation

This section will detail the effects of moisture, temperature and damage accumulation from vehicular loading. The effects that are modeled are:

- Strength(moisture,temperature)
- Modulus(temperature,damage accumulation)
- Remaining Strength(fatigue cycles)

Each individual model was analyzed by adding it to the program individually. The summation of each term was then compared to the combination of all of the effects. It is shown in Figure 51 that the combination has a longer life than the summation of the individual terms. Each of these effects will be analyzed in the following sections.

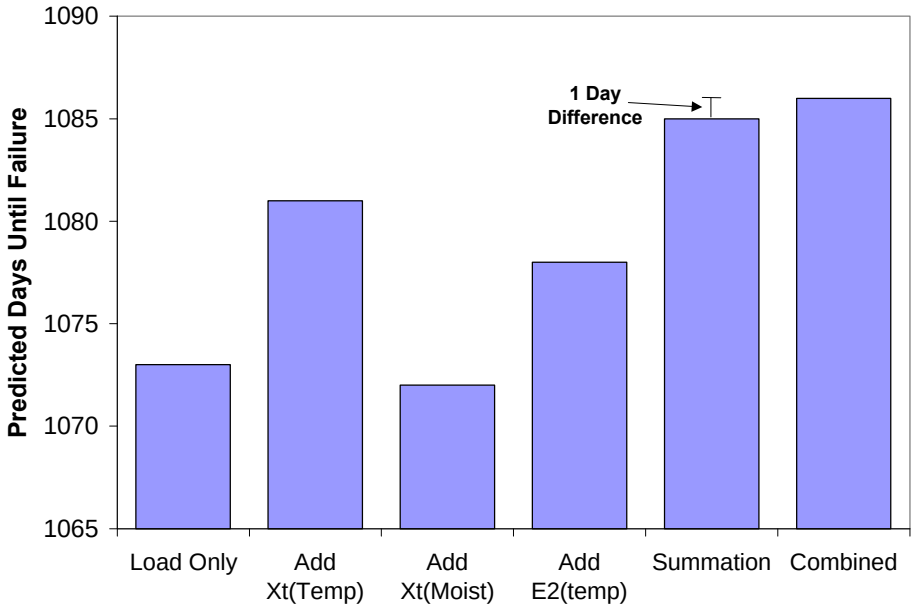

Figure 51. Number of days until failure looking at each condition individually and combined together. The summation of terms is different than the combined effect.

The most significant finding is that there is only a thirteen day difference between the Load Only condition and the Combined condition. Considering the time frame of the prediction, this is a very small difference. This implies that the effects of temperature and moisture are not large factors in the time frame of this prediction. This is not

surprising since the predicted life is just over three years. In order to obtain a larger difference in these conditions, a much greater time frame will be necessary. The author recommends that in order to increase the time frame, a material with a higher ultimate tensile strength be used. A composite with carbon fibers would meet this criterion.

4.6.1. Moisture

The simulation was ran for 1,000,000 days to see how the moisture distribution through the laminate. Using the moisture properties of the quasi-isotropic laminate and the simulated bridge environment, saturation would occur in approximately 164 years (Figure 52). It is interesting to note that the top layer concentration fluctuates, while inner layers don't. Adda-Bedia et al. also noted this effect [50].

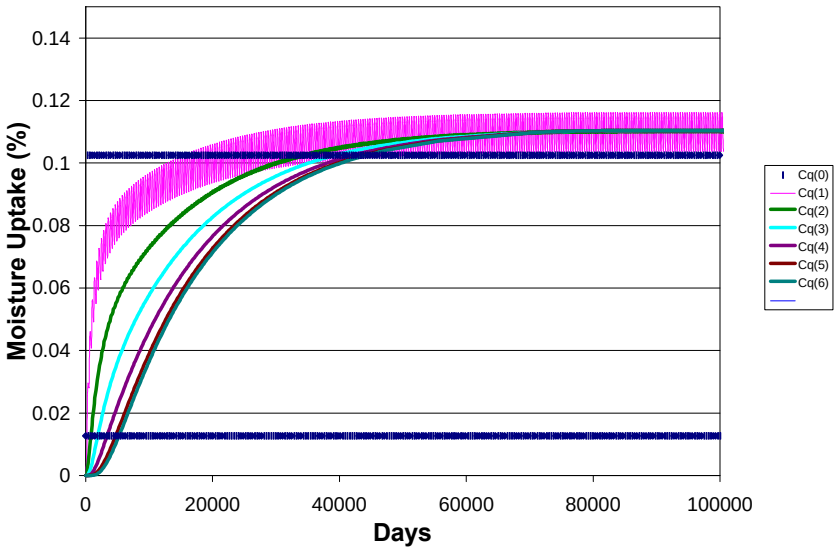

Figure 52. Moisture concentration through the thickness of the composite. Note that the outer layer of shows fluctuation.

Comparing Figure 52 to the predicted lifetime of 1086 days, one can note that there is very little moisture within the composite. Thus it is not surprising that Figure 51only shows a difference of one day between the Load Only and Add Xt(temp) conditions.

4.6.2. Strength (moisture,temperature)

From Figure 51, we observe that adding the strength as a function of temperature model actually increases the life prediction. The strength during the cold winter is stronger than in the hot summer. These colder temperatures actually make the composite stronger, thus increasing the life prediction. As seen in Figure 53, strength is definitely dominated by the change in temperature. Also notice that there is a bend in the change in strength during the spring and fall seasons. This is due to the bi-linear model for strength as a function of temperature. Strength was constant during winter and summer.

The addition of the moisture effects to the program decreased the life prediction by one day. Knowing that moisture saturation occurs in 164 years, one can imagine that only little moisture uptake occurs in three years. Thus, the strength reduction due to moisture is quite small.

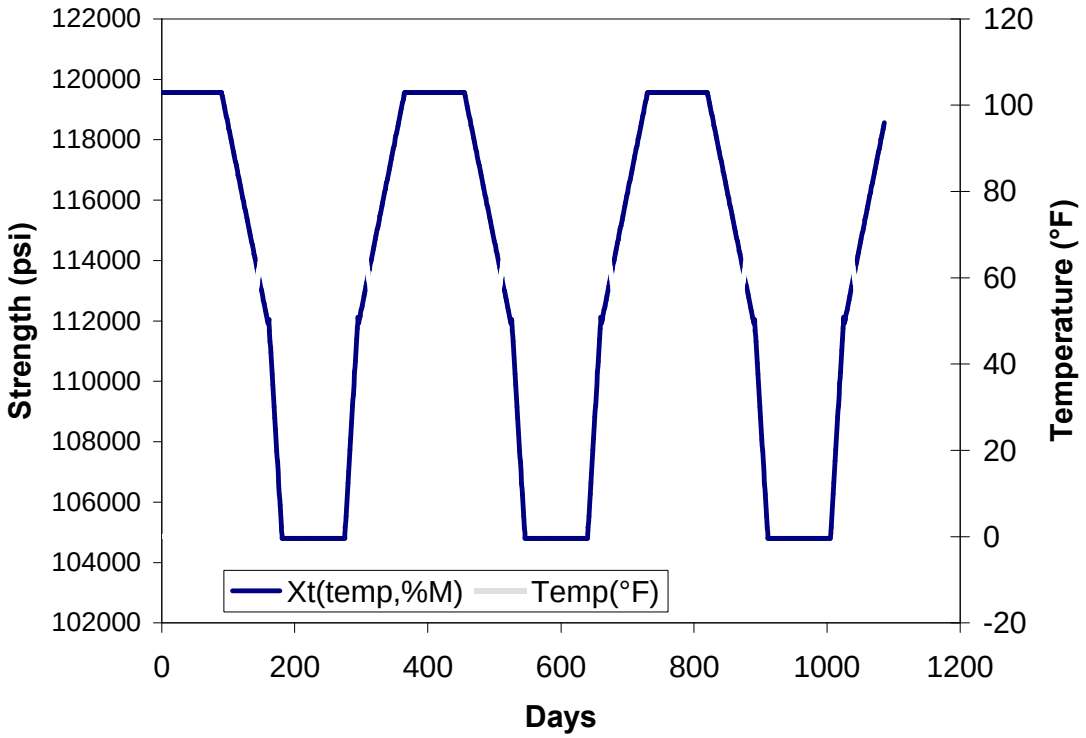

Figure 53. Strength as a function of temperature and moisture.

4.6.3. Modulus (temperature,damage accumulation)

Adding the effect of modulus as a function of temperature also increased the life prediction of the model. The matrix material was modeled as getting stiffer in cold temperatures, thus more load was shared by the off axis plies and less in the 0° fiber direction. The modulus average decreased over the life of the composite due to the damage accumulation model. These results are shown in Figure 54.

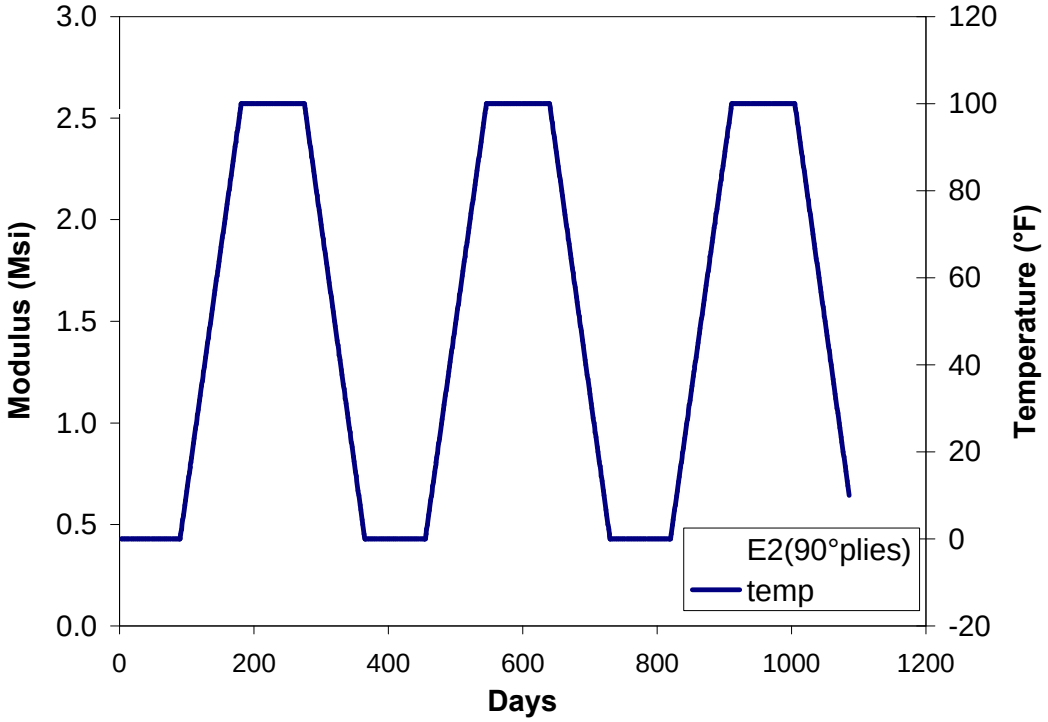

Figure 54. Modulus as a function of temperature and damage accumulation.

4.7. Parametric Study

In order to understand the affects of moisture and temperature on the life of the vinyl ester/E-glass composite, the computer simulation was conducted with varying levels of moisture and temperature. The computer analysis was performed at moisture levels between 0 and 0.5% moisture uptake and temperature levels of 0° to 100° F. Moisture and temperature were held constant for each simulation.

This parametric study shows the affects of moisture and temperature and how they influence the fatigue life. Figure 55 details a parametric study for the vinyl ester/E-glass composite showing the fatigue life at various moisture levels for 0°, 50°, and 100° F using a simulated truck load (load defined in section 4.1.2). From the graph, one can determine that there is not a large change in life between 0° and 100° F and at a constant moisture level, yet there is a considerable change in life between 0 and 0.5% moisture at a constant temperature.

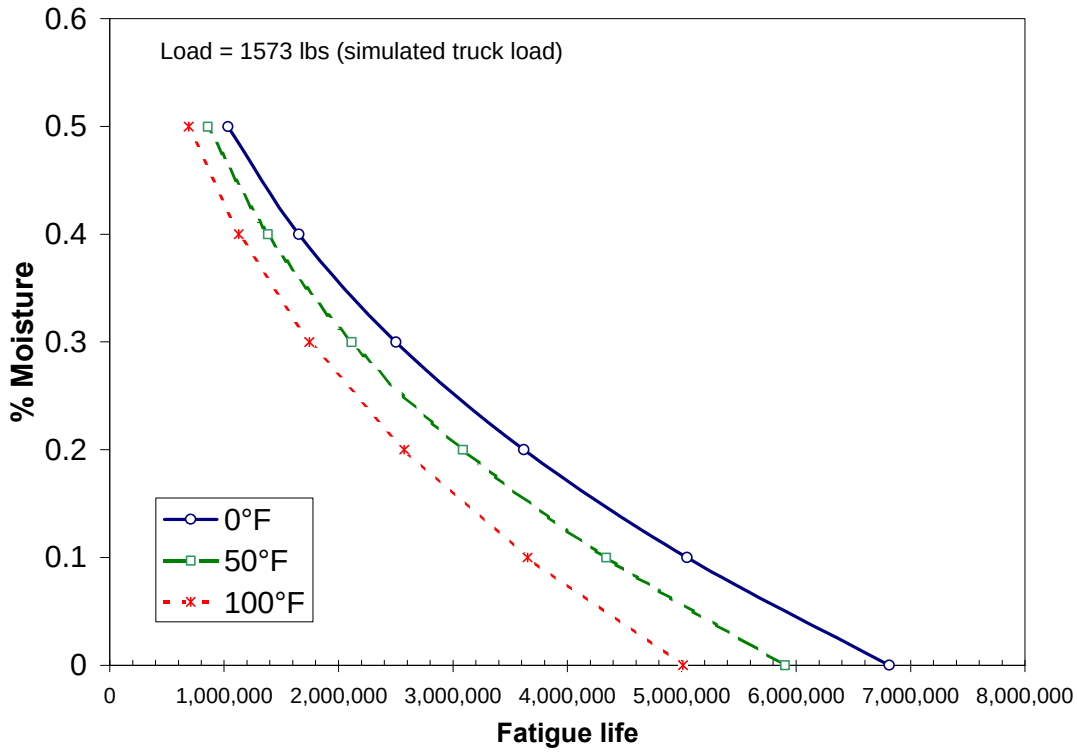

Figure 55. Parametric study for vinyl ester/E-glass composite showing the fatigue life at various moisture levels for 0°, 50°, and 100° F using a simulated truck load.

Parametric studies are also excellent tools for the design engineer. By knowing the environmental conditions, the engineer can determine approximate lifetimes given a maximum moisture and temperature condition.

4.8. Computer Simulation Code

The computer simulation was created in Fortran 90. A copy of the code used in this study can be obtained by contacting Dr. John J. Lesko at:

120 Patton Hall
Blacksburg, VA
24061
(540) 231-5259
jlesko@vt.edu

Chapter 5. Laboratory Simulation of Enviro-mechanical Durability of E-Glass/Vinyl Ester Composites using a Bridge Service Environment

The conditions seen at the Tom's Creek Bridge of Blacksburg, VA was mimicked using an environmental chamber and MTS servo-hydraulic test frame. The conditions seen at the bridge were accelerated, condensing one year into approximately six and a half hours. This section will detail the experimental considerations and results of this study. This study will also be compared to the life prediction outlined in the previous section.

5.1. Experimental Considerations

In order to create an accelerated test, certain assumptions must be made. This section will outline the environmental and mechanical loading considerations used to create an accelerated test that mimics the conditions seen at the Tom's Creek Bridge. Most of these considerations have been outlined in chapter 5.

5.1.1. Vehicle Loading

As stated in chapter 5, the loading of a bridge is highly random and controlled by resident traffic. A vehicle loading study indicated that most of the loading was due to cars and trucks. These two vehicle types were given load values of 3000 pounds and 5000 pounds. Using the equations outlined in chapter 5, this loading was converted to a stress seen on the bottom flange of the bridge beam. This stress was then applied to specimens of quasi-isotropic laminates of vinyl ester/glass composite. Specimen dimensions are 1" wide, .186" thick, and 7 " long. The stresses applied to these specimens are equivalent to 883 lbs and 1573 lbs respectively. Tension-tension fatigue was then used with an R ratio of 0.1.

Instead of writing a computer program to change the loading frequency during the laboratory simulation, a simple load pattern was picked that would mimic that of the bridge. The ratio of truck to car loading was found to be 2:7, thus a repeated block load having two truck loads followed by seven car loads was used (Figure 56). The loading for the laboratory simulation was programmed in a MTS 413 micro-profiler, creating a triangle waveform. The specimens were loaded at a frequency of 14.75 Hz.

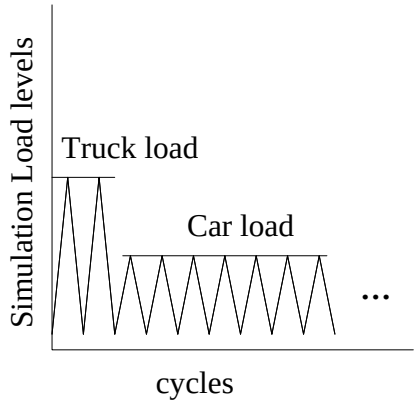

Figure 56. Schematic showing load pattern used in laboratory and computer simulations. A ratio of truck to car loadings is given as 2:7. Truck and car loads defined for the test were 1573 lbs and 883 lbs respectively.

The total number of cars and trucks that pass over the bridge in one day was recorded as 477 vehicles. Since each vehicle has two axles, this equals 954 load cycles in one day or 348,210 cycles in one year. By dividing by the frequency of the test, 14.75 Hz, one year is compressed to 6 hours, 33 minutes, and 11 seconds.

5.1.2. Humidity and Temperature

A Russells environmental chamber was attached to the MTS test frame. The chamber had the ability to change humidity and temperature. The same scenario for humidity and temperature in chapter 5 was again utilized here. Winters and summers were given constant temperatures of 0° and 100° F and relative humidity of 0% and 90% RH respectively. Spring and Fall were defined as transition regions with relative humidity of 70% RH. The time frame of this "year" cycle was 6 hours, 33 minutes, and 11 seconds.

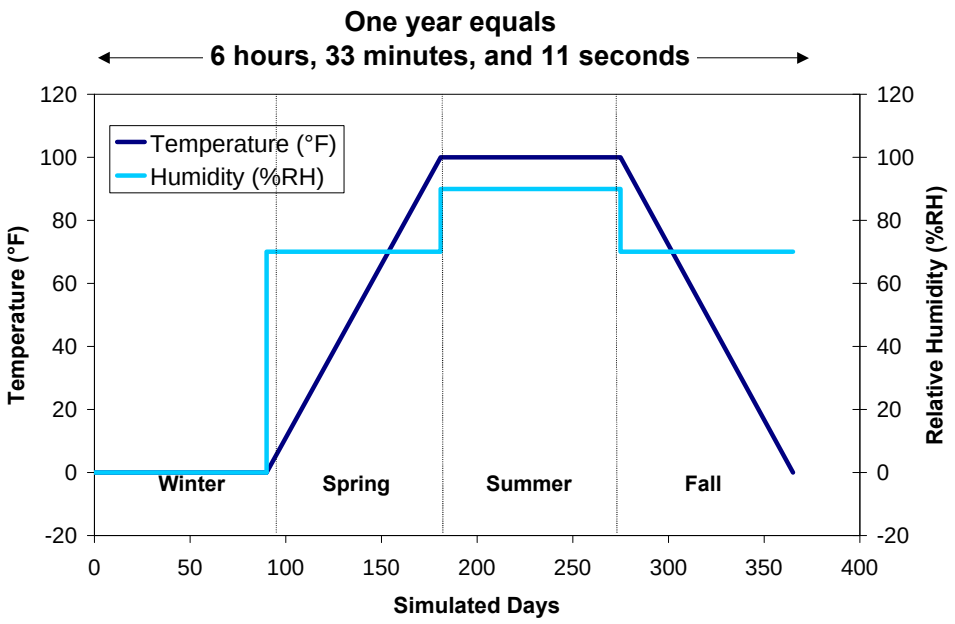

Figure 57. Schematic showing humidity and temperature used in the laboratory simulation. One year is condensed to 6 hours, 33 minutes, and 11 seconds.

5.2. Results: Comparison of Computer and Laboratory Simulations

The laboratory simulation, using the enviro-mechanical pattern described, was conducted until failure of the vinyl ester/glass composite. The test was started with a summer environmental condition. Failure was seen at a little over six years, with failure occurring during the summer season. Remaining strength specimens were fatigued for one, three, and five simulated years with quasi-static tensile tests conducted at room temperature. The results were then compared to the life prediction using the critical element model that was detailed in chapter 5. The results are seen in Figure 58. The prediction fits the experimental data quite well, and gives a moderately conservative estimate of failure life with these given environmental conditions.

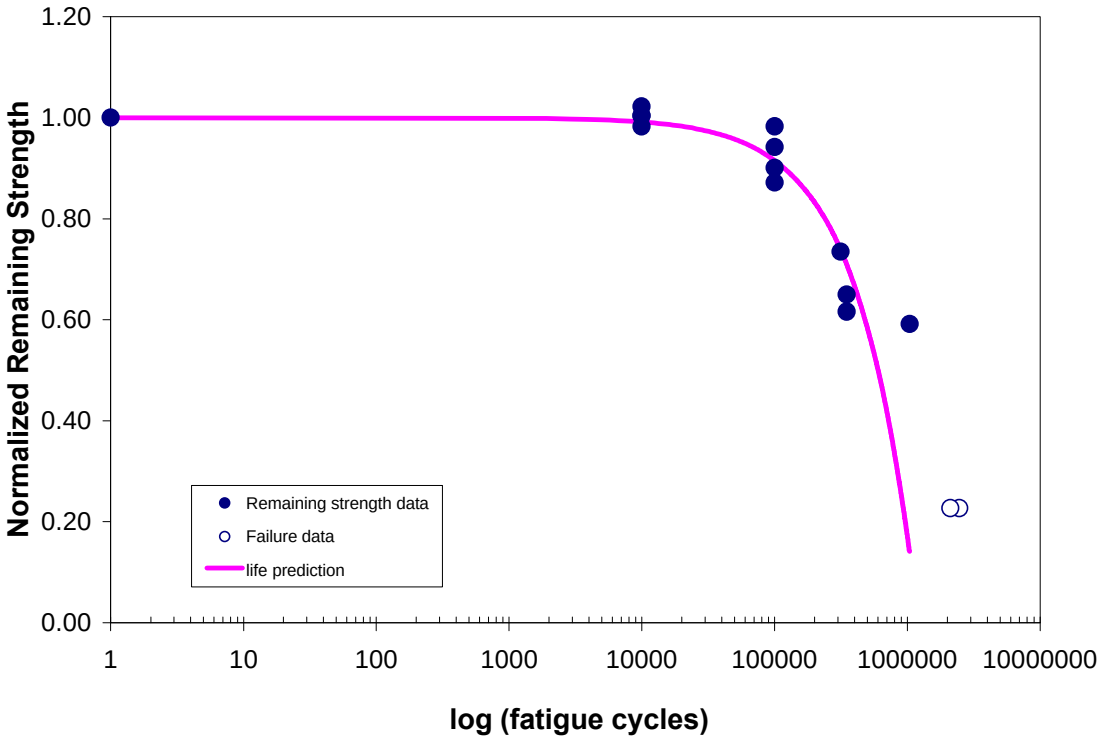

Figure 58. Comparison of life prediction and laboratory simulation data.

One interesting feature of the failure data points is the season that failure occurs in. The data points for failure correspond to 6 years, 26 days and 7 years 26 days. Since the simulation was started at summer environmental conditions, this meant that both failures occurred in the mid to early summer when temperature is the warmest. As temperature increases, the strength of the composite decreases, thus the failures occurred when the composite was in its weakest form. At first glance, the predicted failure of 2 years, 356 days seems extremely conservative. Considering the numbers in log time, one finds that the difference is only $1/10^{th}$ of a decade. This is quite accurate in terms of fatigue life.

Table 4. Laboratory Simulation and Predicted Failure Times

Specimen	Simulated failure time		Failure cycles
1	6 years	26 days	2114352
2	7 years	26 days	2462544
predicted	*2 years*	*356 days*	*1036044*

Chapter 6. Summary and Conclusions

This thesis focuses on the development of a life prediction model for use with fiber reinforced polymer composites in bridge service environments. The environmental conditions of moisture and temperature are modeled to simulate conditions seen at the Tom's Creek Bridge of Blacksburg, VA. The stresses from vehicular loading of a composite beam were converted to approximate tensile loads for a $(0/90/(^{+}_{-}45)_2/0/90)_{2T}$ laminate of vinyl ester/glass composite. The individual effects of temperature, moisture and vehicular loading were then used to create a life prediction model based on the critical element model. Finally, a laboratory simulation is conducted that models the temperature, humidity, and a multi-stress load pattern that represents conditions at the Tom's Creek Bridge, but in an accelerated time frame. Using a servo-hydraulic test frame and environmental chamber, one year of conditions is accelerated to approximately six hours and thirty-three minutes.

6.1. Summary

The following summarizes the investigations conducted within the scope of this thesis.

1. Investigations were made to determine material response to temperature, moisture and multi-stress loading.
   - Moisture uptake studies were done at 95°, 113°, 131°, and 149° F in water. Results of the moisture uptake studies were able to be modeled using Fick's Law of Diffusion. Initial slopes of the moisture uptake curves were used to determine activation energy and diffusion coefficient. The Arrehnius equation for this particular vinyl ester/glass composite system is:

$$D = .0330e^{-3527/RT}$$

- Tensile tests were done on specimens that had been aged at 149° F in water at 0.15, 0.30, 0.45, and 0.60% relative moisture content. The results showed an increase in strength at 0.15% moisture content followed by a decrease in tensile strength with increasing moisture. The initial increase is possibly due to increased cure from the aging temperature or residual stress relief from matrix swelling.
- Iso-moisture studies were conducted to determine if aging temperature had an effect on tensile properties. Specimens were aged at 95°, 113°, 131°, and 149° F in water until 0.30% relative moisture was achieved. Results of the iso-moisture study concluded that aging temperature did not have a significant effect on the tensile strength of the vinyl ester/glass composite.
- Fatigue testing was conducted on composites that were aged in water at 149° F until 0.60% moisture was reached. Tests were conducted using a fluid cell that kept the gage section in constant contact with water. Water temperature was kept at 86° F. Results showed a 10.6% decrease in strength per decade of life. This correlates well with Mandell's 10-11% decrease per decade for glass fiber composites.
- Quasi-static tensile tests were done at 0°, 25°, 50°, 75°, and 100° F to determine tensile properties as a function of temperature. The results show a decrease in strength with temperature. A linear fit shows a .135% change per degree Fahrenheit, thus over the 100° F range, a 13.5% change is seen.
- Cyclic temperature tests were performed on the vinyl ester/glass composite between 0° and 100° F on loaded and unloaded specimens. Results showed that cyclic temperature between 0° and 100° F on this composite system shows no change in strength up to 1000 temperature cycles.
- The effects of multi-stress block loading were evaluated with good correlation to the critical element model and Miner's Rule. Both the critical element model and Miners rule predicted conservative results for the high-low condition but over predicted the low-high scenario.

2. A life prediction scheme was created using the service conditions of the Tom's Creek Bridge of Blacksburg, VA.
    - The critical element model was used to track remaining strength as a function of fatigue cycles. Damage accumulation was defined by off-axis stiffness reduction caused from matrix cracking.
    - Due to changing boundary conditions, moisture was modeled using the finite difference method. Temperature was defined by the seasons of the year. Winter and summer were constant temperatures of 0° and 100° F. Spring and summer were transition ramps between winter and summer.
    - The computer simulation predicted that failure would occur in 1,034,044 simulated vehicle cycles, or in 2 years, 356 days.
    - The different environmental components were individually added to the computer simulation and compared to the total affect of all components. A significant discovery was that there was little change between the simulation with and without environmental components. Moisture did not have an affect since the short time frame did not allow for a large moisture concentration. Temperature also showed little affect on predicted fatigue life.

3. Finally, the conditions of the bridge were mimicked in a laboratory environment. The results were compared to the life prediction.
    - The laboratory simulation was able to accelerate the service conditions of one year into 6 hours and 33 minutes.
    - The same temperature, humidity, and load pattern used in the computer simulation were used in the laboratory simulation.
    - Two tests were completed with failures occurring at 2,114,352 and 2,462,544 simulated vehicle cycles, or in 6 years 26 days and 7 years 26 days. For both cases, failure occurred in the summer where higher temperatures decreased the strength of the material.

6.2. Conclusions

This thesis developed a life prediction model for use with fiber reinforced polymer composites in bridge service environments. This was accomplished by creating a computer simulation based on the conditions seen at the Tom's Creek Bridge of Blacksburg, VA. A laboratory simulation was performed that validated the findings of the computer simulation. The results showed that life prediction of vinyl ester/E-glass composites, using the remaining strength approach, gave conservative estimates when compared to the laboratory simulations. Also, the affects of temperature and moisture were minimal. Moisture did not have an affect since the short time frame did not allow for a large moisture concentration.

Chapter 7. Recommendations for Future Work

The following are some recommendations for future work:

1. A spectral, or random, loading would better mimic the loading seen on the Tom's Creek Bridge. The current analysis uses a small block-loading scheme with two loads.
2. An independent analysis showed that cars driving over the Tom's Creek Bridge had approximately a 1 Hz load frequency. Thus, slowing the loading to 1 Hz is another way to simulate the bridge loading. This would also increase moisture absorption during the test.
3. The current material is a vinyl ester/glass composite where the Tom's Creek Bridge is a hybrid of glass and carbon fibers in a vinyl ester matrix. A better model for use with the Tom's Creek Bridge would be with a hybrid composite material.
4. The most common failure mode in beams used in bridges is delamination, not tensile failure of the bottom flange. Thus, incorporating a model that uses out of plane failure modes, such as one described by J. Senne [51], would be a more accurate description of life.

REFERENCES

[1] A.H. Zureick, B. Shih, E. Munley, "Fiber-Reinforced Polymeric Bridge Decks," *Structural Engineering Review*, vol. 7, no. 3, p 257, 1995

[2] "Composite Structural Shapes for Infrastructure," National Institute of Standards and Testing (NIST), Advanced Technology Program, 1994

[3] "Partnership for the Advancement of Infrastructure and Its Renewal Transportation Component (PAIR-T) Technology and Investment Plan White Paper," The Civil Engineering Research Foundation, Washington, DC, Spring-Summer 1998

[4] B. Brailsford, S.M. Milkovich, D.W. Prine, J.M. Fildes, "Definition of Infrastructure Specific Markets for Composite Materials: Topical Report," Northwestern University BIRL Project P93-121/A573, July 11, 1995

[5] M. Hayes, "Characterization and modeling of a Fiber-Reinforced Polymeric Composite Structural Beam and Bridge Structure for Use in the Tom's Creek Rehabilitation Project," Masters Thesis, Dept. of Engineering Science and Mechanics, Virginia Polytechnic Institute and State University, February, 1998

[6] G.S. Springer, "A Model for Predicting the Mechanical Properties of Composites at Elevated Temperatures," *Journal of Reinforced Plactics and Composites,* Vol. 3, p 85, 1984

[7] C.H. Shen and G.S. Springer, "Moisture Absorption and Desorption of Composite Materials," Environmental Effects on Composite Materials, Vol. 1, Technomic Publishing Co., Westport, CT, p 15, 1981

[8] A.C. Loos and G.S. Springer, "Moisture Absorption of Graphite-Epoxy Composition Immersed in Liquids and in Humid Air," Environmental Effects on Composite Materials, Vol. 1, Technomic Publishing Co., Westport, CT, p 34, 1981

[9] A.C. Loos and G.S. Springer, "Effects of Thermal Spiking on Graphite-Epoxy Composites," Environmental Effects on Composite Materials, Vol. 1, Technomic Publishing Co., Westport, CT, p 108, 1981

[10] A.C. Loos, G.S. Springer, B.A. Sanders, and R.W. Tung, "Moisture Absorption of Polyester-E Glass Composites," Environmental Effects on Composite Materials, Vol. 1, Technomic Publishing Co., Westport, CT, p 51, 1981

[11] G.S. Springer, "Moisture Content of Composoites Under Transient Conditions," Environmental Effects on Composite Materials, Vol. 1, Technomic Publishing Co., Westport, CT, p 63, 1981

[12] G.S. Springer, "Numerical Procedures for the Solution of One-Dimensional Fickian Diffusion Problems," Environmental Effects on Composite Materials, Vol. 1, Technomic Publishing Co., Westport, CT, p 166, 1981

[13] C.H. Shen and G.S. Springer, "Effects of Moisture and Temperature on the Tensile Strength of Composite Materials," Environmental Effects on Composite Materials, Vol. 1, Technomic Publishing Co., Westport, CT, p 79, 1981

[14] C.H. Shen and G.S. Springer, "Environmental Effects on the Elastic Moduli of Composite Materials," Environmental Effects on Composite Materials, Vol. 1, Technomic Publishing Co., Westport, CT, p 94, 1981

[15] G.S. Springer, B.A. Sanders and R.W. Tung, "Environmental Effects on Glass Fiber Reinforced Polyester and Vinylester Composites," Environmental Effects on Composite Materials, Vol. 1, Technomic Publishing Co., Westport, CT, p 126, 1981

[16] S.N. Singhal and C.C. Chamis, "Environmental Effects on Long Term Behavior of Composite Laminates," *International SAMPE Electronics Conference*, Vol. 24, p 852, 1992

[17] P.R. Ciriscioli, W.I. Lee, D.G. Peterson, G.S. Springer, and J. Tang, "Accelerated Environmental Testing of Composites," *Journal of Composite Materials*, Vol. 21, p 225, 1987

[18] S. Sridharan, "Environmental Durability of E-Glass/Vinylester Composites in Hot-Moist Conditions," Doctorate Thesis, Georgia Institute of Technology, September, 1997

[19] A. Chateauminois, B. Chabert, J.P. Soulier, and L. Vincent, "Hygrothermal Ageing Effects on the Static Fatigue of Glass/Epoxy Composites," *Composites*, Vol. 24, p 547, 1993

[20] D. Jungk, F. McBagonluri, M.Hayes, and J.J.Lesko, "Fatigue Behavior of High Performance Polymeric Composites in a Simulated Sea Environment," Report to the National Institute of Standards and Technology, 1999

[21] J. Gomez and B. Castro, "Freeze-Thaw Durability of Composite Materials," *Fiber Composites in Infrastructure*, Proceedings of the First International Conference on Composites in Infrastructure, 1996, p 947

[22] P.K. Dutta, "A Micromechanical Study of the Freeze-Thaw Behavior of Polymer Composites," *The Proceedings of the 7th International Offshore and Polar Engineering Conference*, 1997, p 672

[23] J. Haramis, "Freeze-Thaw Durabilty of Polymeric Composite Materials for Use in Civil Infrastructure," Doctorate Dissertation, Dept. of Civil Engineering, Virginia Polytechnic Institute and State University, Yet to be published

[24] S. Phifer, "Quasi-Static and Fatigue Evaluation of Pultruded Vinyl Ester/E-Glass Composites," Masters Thesis, Dept. of Engineering Science and Mechanics, Virginia Polytechnic Institute and State University, December, 1998

[25] J.F. Mandell, "Fatigue Behavior of Fibre-Resin Composites," *Developments in Reinforced Plastics 2, Properties of Laminates,* 1978

[26] J.F. Mandell, D. Huang, and F.J. McGarry, Proceedings of the 37th Conference on Reinforced SPI/CI, paper 23C, 1982

[27] Hartman, D.R., Greenwood, M.E., and Miller, D.M., "High Strength Fibers", Technical Paper by Owens Corning, 1991

[28] S. Phifer, "Temperature-Moisture-Mechanical Response of Vinyl Ester Resin and Pultruded Vinyl Ester/E-glass Laminated Composites,"

[29] C. Henaff-Gardin, M. C. Lafarie-Frenot and D. Gamby, "Doubly periodic matrix cracking in composite laminates. Part 1: general in plane loading," *Composite Structures* Vol. 36, p 113, 1996.

[30] C. Henaff-Gardin, M. C. Lafarie-Frenot and D. Gamby, "Doubly periodic matrix cracking in composite laminates. Part 2: thermal biaxial loading." *Composite Structures,* Vol. 36, p 131-140, 1996

[31] G-P. Fang, R.A. Schapery, and Y. Weitsman, "Thermally-induced Fracture in Composites," *Engineering Fracture Mechanics,* Vol. 33, No. 4, p 619, 1989

[32] I. Emri, and V. Pavsek, "On the Influence of Moisture on the Mechanical Properties of Polymers," *Materials Forum*, Vol. 16, p 123, 1992

[33] O. Gilat and S.S. Broutman, "Effect of an External Stress on Moisture Diffusion and Degredation in Graphite-Reinforced Epoxy Laminates, Advanced Composite Materials – Environmental Effects," ASTM, STP-658, J.R. Vinson, ed., 1978, p 61

[34] G. Yaniv, and O. Ishai, "Coupling between Stresses and Moisture Diffusion in Polymeric Adhesives," *Polymer Engineering and Science,* Vol. 27, p 731, 1987

[35] K.N.E. Verghese, M.D. Hayes, K. Garcia, C. Carrier, J. Wood, J.R. Riffle, and J.J. Lesko, "Influence of Matrix Chemistry on the Short Term, Hydrothermal Aging of Vinyl Ester Matrix and Composites Under Both Isothermal and Thermal Spiking Conditions," *Journal of Composite Materials,* Vol. 33, No. 20, 1999, p 1918

[36] L.W. Cai, and Y. Weitsman, "Non-Fickian Moisture Diffusion in Polymeric Composites," *Journal of Composite Materials*, Vol. 28, p 130, 1994

[37] M. Blikstad, P.O.W. Sjoblom, and T.R. Johannesson, "Long-Term Moisture Absorption in Graphite/Epoxy Angle-Ply Laminates," *Journal of Composite Materials*, Vol. 18, p 32, 1984

[38] M.A. Miner, "Cumulative Damage in Fatigue", Journal of Applied Mechanics, vol. 12, p A159, 1945

[39] N. Gathercole, H. Reiter, T. Adam, and B. Harris, "Life Prediction for Fatigue of T800/5245 Carbon-Fibre Composites: I. Constant-amplitude Loading," International Journal of Fatigue, vol. 16, p 523, 1994

[40] T. Adam, N. Gathercole, H. Reiter, and B. Harris, "Life Prediction for Fatigue of T800/5245 Carbon-Fibre Composites: II. Variable-amplitude Loading," International Journal of Fatigue, vol. 16, p 533, 1994

[41] A. Zago, G.S. Springer, and M. Quaresimin, "Cumulative Damage of Short Glass Fiber Reinforced Thermoplastics," Journal of Reinforced Plastics and Composites, Yet to be published

[42] A. Zago, and G.S. Springer, "Fatigue Lives of Short Fiber Reinforced Thermoplastics Parts," Journal of Reinforced Plastics and Composites, Yet to be published

[43] S.M. Marco, and W.L. Starkey, "Cumulative Fatigue Damage," Proceedings of the International Conference on Fatigue of Metals, IME and ASME, 1956

[44] L.J. Broutman, and S. Sahu, "A new theory to predict cumulative fatigue damage in fiberglass reinforced plastics," Composite Materials: Testing and Design (Second Conference), ASTM STP 497, p. 170, 1970

[45] K.L. Reifsnider, and W.W. Stinchcomb, "A Critical Element Model of the Residual Strength and Life of Fatigue-Loaded Composite Coupons," *Composite Materials: Fatigue and Fracture,* ASTM STP 907, Edited by H.T. Hahn, ASTM, Philadelphia, PA, 1986

[46] H.T. Hahn and S.W. Tsai, "On the Behavior of Composite Laminates after Initial Failures," *Journal of Composite Materials*, Vol. 8, p 288, 1974

[47] K.L. Reifsnider, E.G. Henneke, and W.W. Stinchcomb, "Defect-Property Relationships in Composite Materials," AFML-TR-76-81, Part IV. Air Force Materials Laboratory, June, 1979

[48] K.L. Reifsnider, "Some Fundamental Aspects of Fatigue and Fracture Response of Composite Materials," Proceedings, 14th Annual Meeting of Society of Engineering Science, Lehigh University, Bethlehem, PA, Nov. 1977

[49] P.K. Aditya and P.K. Sinha, “Diffusion Coefficients of Polymeric Composites Subjected to Periodic Hygrothermal Exposure,” *Journal of Reinforced Plastics and Composites*, Vol. 11, p 1035, 1992

[50] E. Adda-Bedia, W.S. Han, G. Verchery, “Simplified Methods for Prediction of Moisture Diffusion in Polymer Matrix Composites with Cyclic Environmental Conditions” *Polymer and Polymer Composites*, Vol. 6, p 189, 1998

[51] J. Senne, “Fatigue Life of Hybrid FRP Composite Beams,” Masters Thesis, Dept. of Engineering Science and Mechanics, Virginia Polytechnic Institute and State University, 2000

VITA: David Alan Jungkuist

The author was born August 20, 1975 in Manson, Washington to parents Larry and Terry Jungk. He graduated from Manson High School in 1993 as valedictorian and senior class president. He then pursued a bachelor's degree in Materials Science and Engineering at Washington State University, graduating caume laude in 1998. He also earned the prestigious Outstanding Senior in Engineering and Architecture award. While at Washington State University, David focused his studies on polymer and composite engineering. During a summer research program for W.S.U., he designed and developed an undergraduate polymer lab that is currently part of the curriculum. Another focus of his undergraduate career was running for the varsity track and cross country teams. He was elected captain of the cross country team his senior year, leading the school to a 11^{th} national ranking. During the summer of 1997, David was a participant in the summer undergraduate research program at Virginia Tech researching the phenomena of physical aging on poly ether ether ketone. After graduation from Virginia Tech, David plans on working in industry in the field of composite materials.